Forecasting of Irradiance on Bifacial Solar Panel based on Climate Parameters and Tilt Angle

Author

JUNAID IQBAL

Registration Number

362035

Supervisor

DR. MUHAMMAD SAJID

DEPARTMENT OF MECHANICAL ENGINEERING

SCHOOL OF MECHANICAL & MANUFACTURING ENGINEERING

NATIONAL UNIVERSITY OF SCIENCES AND TECHNOLOGY

ISLAMABAD

APRIL, 2023

Forecasting of Irradiance on Bifacial Solar Panel based on Climate
Parameters and Tilt Angle

Author

JUNAID IQBAL

Registration Number

362035

A thesis submitted in partial fulfillment of the requirements for the degree of

MS Mechanical Engineering

Thesis Supervisor:

DR. MUHAMMAD SAJID

Thesis Supervisor's Signature: _____

DEPARTMENT MECHANICAL ENGINEERING

SCHOOL OF MECHANICAL & MANUFACTURING ENGINEERING

NATIONAL UNIVERSITY OF SCIENCES AND TECHNOLOGY,

ISLAMABAD

APRIL, 2023

<u>**Certificate for Plagiarism**</u>

Plagiarism Certificate (Turnitin Report)

This thesis has been checked for Plagiarism. Turnitin report endorsed by Supervisor is attached.

Signature of Student

JUNAID IQBAL

Registration Number 362035

Signature of Supervisor

Declaration

I certify that this research work titled "*Forecasting of Irradiance on Bifacial Solar Panel based on Climate Parameters and Tilt Angle*" is my own work. The work has not been presented elsewhere for assessment. The material that has been used from other sources it has been properly acknowledged / referred.

Signature of Student

JUNAID IQBAL

2021-NUST-Ms-Mech-362035

Copyright Statement

Acknowledgements

I express gratitude to Allah Subhana-Watala, the Almighty, for guiding me throughout this work and providing me with new thoughts to enhance it. Without His invaluable assistance and direction, I could not have accomplished anything. Any individual who supported me during my thesis, be it my parents or others, was in accordance with His will. Therefore, all praise belongs to Allah alone.

I express my heartfelt gratitude to my dear parents who provided me with unconditional care and support from the time I was an infant, and continued to guide and assist me in all aspects of my life.

I extend my sincere gratitude to my supervisor, Dr. Muhammad Sajid, for his constant support and guidance during my thesis. Additionally, I would like to acknowledge his exceptional teaching of Modelling & AI course. The motivation and knowledge that I have gained from his instruction is unparalleled in any other engineering subject.

I would like to express my profound gratitude to my supervisor, whose unwavering support and cooperation were integral to the successful completion of my thesis. His invaluable assistance was indispensable in overcoming any obstacles I encountered. I cannot thank him enough for his unyielding patience and guidance throughout the entire thesis.

My supervisor's exceptional mentorship and encouragement were instrumental in bringing my thesis to fruition. I am deeply grateful for his steadfast dedication to helping me navigate through the complexities of the research process. His astute insights and timely feedback have been invaluable in shaping my work. I could not have asked for a more knowledgeable, understanding, and supportive guide.

I extend my sincere appreciation to Dr. Sara Baber and Dr. Khawaja Fahad Iqbal for their invaluable contributions as members of my thesis guidance and evaluation committee. Their expertise and insights were instrumental in shaping the direction and scope of my research. Additionally, I would like to express my gratitude to Wajahat Iqbal and Faizan Faiz for their unwavering support and cooperation throughout the thesis process.

Lastly, I am deeply grateful to all the individuals who have provided me with valuable assistance in my study. Their contributions have been invaluable in helping me achieve my research goals, and I am truly thankful for their support.

I dedicate this wonderful accomplishment to my exceptional parents and adored siblings, whose unwavering support and cooperation have been instrumental in making it possible. Their encouragement, guidance, and sacrifices have been invaluable in shaping my academic journey, and I could not have reached this milestone without them.

Abstract

The aim of this study was to explore the use of data-driven approaches for designing net zero energy buildings using bifacial solar panels and deep learning models. The study utilized historical data on solar irradiance to forecast future irradiation levels, which were then used to optimize the tilt angle of bifacial solar panels for maximum energy collection. Two deep learning models, namely RNN-LSTM and transformers, were evaluated using various evaluation metrics, including MAE, RMSE, SMAPE, and R2. The results showed that both models were effective in forecasting irradiations with varying forecasting horizons, with the transformers model outperforming the RNN-LSTM model in terms of MAE values. The study provides insights into the use of data-driven approaches for designing net zero energy buildings, highlighting the potential of deep learning models in optimizing the use of renewable energy sources for sustainable development. The results show that both models were effective in forecasting irradiance, with R2 values of 0.927 for RNN-LSTM and 0.894 for Transformers. Additionally, the Transformers model outperformed the RNN-LSTM model with a lower range of MAE values from 0.05 to 0.03 across the same horizons. These findings suggest that deep learning models can effectively forecast solar irradiance and aid in optimizing the performance of net-zero energy buildings.

Key Words: *Net zero energy buildings, Solar irradiance forecasting, Deep learning, RNN-LSTM, Transformer, Bayesian optimization*

Table of Contents

List of Figures

List of Tables

CHAPTER 1: INTRODUCTION

The global energy demand has been growing rapidly over the past few decades, and traditional energy sources such as fossil fuels have been the primary source to meet this demand. However, the use of fossil fuels has caused significant environmental damage due to the emission of greenhouse gases and other pollutants. The carbon emissions from burning fossil fuels are a major contributor to global warming and climate change, which is threatening the sustainability of the planet. The need to reduce carbon emissions has become a pressing issue, and many countries have taken steps to transition towards cleaner and more sustainable energy sources.

The finite nature of fossil fuels has also highlighted the need for a more diverse and sustainable energy mix. The increasing demand for energy worldwide has led to the exploration of new and innovative technologies to meet this demand. Renewable energy sources, such as wind, solar, hydro, and geothermal energy, have emerged as a promising alternative to traditional energy sources. They are clean, abundant, and can be harnessed without depleting natural resources.

Moreover, net-zero energy buildings have also emerged as a potential solution to contribute to a more sustainable future. These buildings are designed to generate as much energy as they consume, thus reducing their carbon footprint significantly. They use a combination of energy-efficient technologies and renewable energy sources to achieve this goal. The environmental impact of traditional energy sources and the need to combat climate change has highlighted the importance of a diverse and sustainable energy mix. The growing demand for energy worldwide, coupled with the limited availability of fossil fuels, has led to the exploration of renewable energy sources. In practical applications, Electromagnetic Radiation encompasses a broad spectrum of wavelengths. This spectrum, known as the Electromagnetic Spectrum, includes gamma rays, X-rays, ultraviolet radiation, visible light, infrared radiation, thermal radiation, microwaves, and radio waves. Gamma rays are generated through nuclear reactions, while X-rays are produced by bombarding metals with high-energy electrons. Special types of electron tubes such as klystrons and magnetrons are used to detect microwaves.
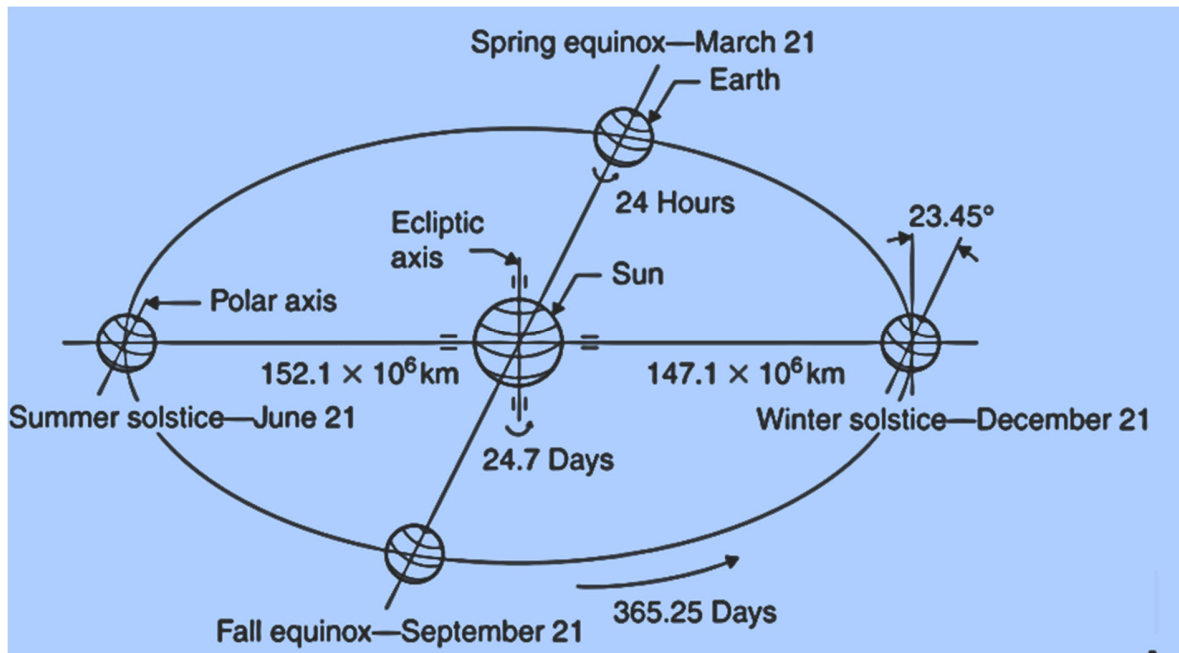
Figure 1: Earth's rotational axis and representation of tilt

The Earth's rotation axis shown in figure 1 is tilted at an angle of 23.45° with respect to the perpendicular to the ecliptic plane. As a result, the angle between the Sun and any given point on the Earth's surface varies throughout the year, leading to changes in the length of day. The rotation of the Earth is responsible for the occurrence of day and night, while its tilt is responsible for the change of seasons.

The Solar Constant G_{sc} refers to the amount of energy that is received from the Sun, per unit time, on a unit area of surface that is maintained perpendicular to the direction of radiation. This occurs at a mean Earth-Sun distance, outside of the Earth's atmosphere.
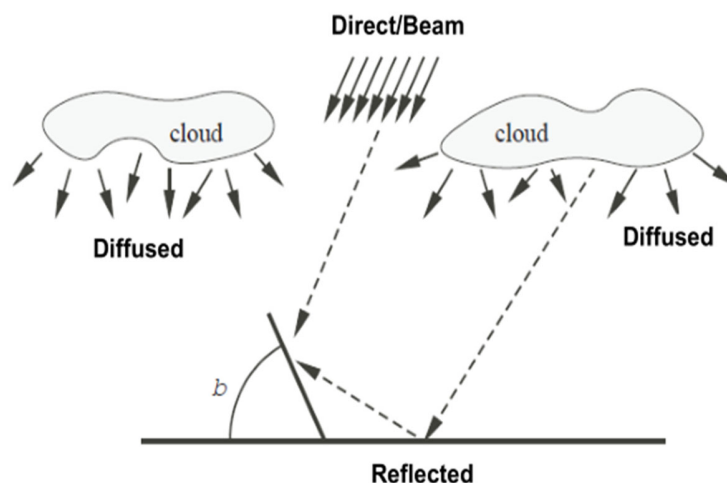
Figure 2: Components of Radiation

Direct Radiation or Beam Radiation are Solar radiation that reaches the Earth's surface directly without being scattered by the atmosphere is known as Direct Radiation. Diffuse Radiation, on the other hand, occurs when radiation is reflected, absorbed, or scattered, but not completely lost in the atmosphere, and is thus able to reach the Earth's surface in the Short Wavelength Region. Global or Total Radiation refers to the sum of diffuse and direct radiation that reaches the Earth's surface. Reflected Radiation, on the other hand, consists of shortwave radiation that is reflected from other surfaces as shown in figure c. Our focus is on the portion of Electromagnetic Radiation emitted from the Sun within the wavelength range of 0.25 – 3.0micron. This is affected by Solar Geometry, which refers to the position of the Sun in the sky and the direction of direct (beam radiation) on various inclined and oriented surfaces. Extraterrestrial radiation on a horizontal surface represents the limit of solar radiation that can be received on the Earth's surface. The Availability of solar radiation is also affected by Earth motion, orientation, and tilt with respect to the Sun. The Earth's atmosphere plays a critical role in reducing solar radiation through Absorption, Scattering, and Reflection.

Angle between the sun's rays or Beam Radiation and the normal to the surface is under our consideration which is known as incidence angle. The angle of incidence θ depends on various factors such as the location on Earth, time of day, day of the year, and surface tilt. When the surface area is not perpendicular to the sunbeam (i.e., zenith angle is not zero), a larger area is needed to catch the same flow as the cross-section of the sunbeam. The amount of solar energy collected in the collectors is strongly influenced by the β values. Optimum slopes for surfaces are affected by different declinations experienced throughout the year. The best slopes are obtained when the solar incidence angle θ is zero at solar noon, as the Sun's rays are normal to the surface. Our goal is to receive the maximum amount of sunlight each day and throughout the year.
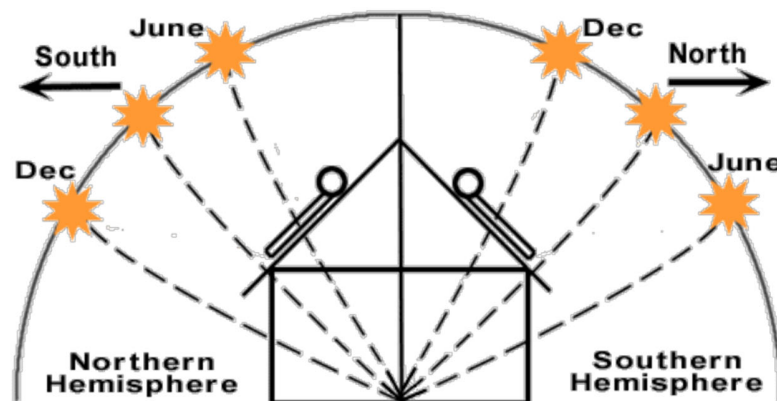
Figure 3: Southern and Northern Hemisphere

The angle and direction of installation of a solar panel is crucial as it greatly impacts the efficiency of solar energy collection. The fixed surface tilt should be oriented correctly to ensure maximum energy collection. For locations in the Northern Hemisphere, the surface should face South while for locations in the Southern Hemisphere, the surface should face North. If the surface is not facing due South, the highest amount of collection will occur either in the morning or afternoon rather than at solar noon, leading to a reduction in the daily total of collected energy as shown in figure 3.
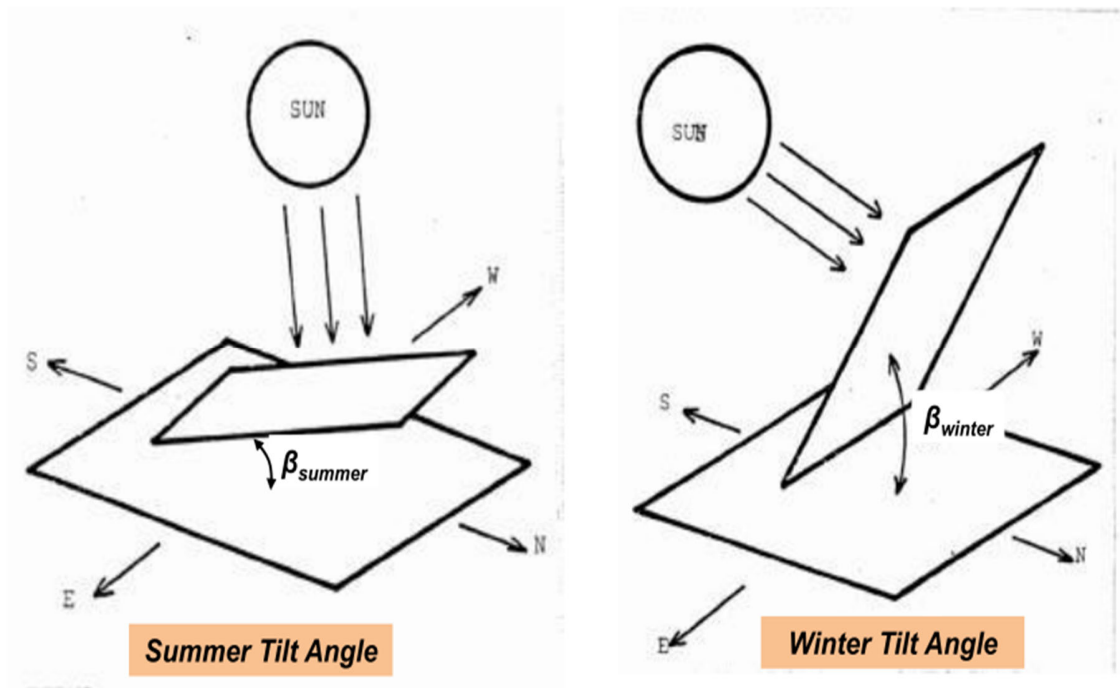
Figure 4: Effect of weather on tilt angle

Slopes for maximizing energy capture for Northern Hemisphere latitudes when $(\varphi - \delta) > 0$ are in such a way that if declination angle is positive than the tilt angle will be the difference of the latitude and declination angle, if the declination angle is zero than the tilt angle will be simply equal to the latitude in figure 4.

Bifacial solar modules, also known as double-sided solar panels, are photovoltaic (PV) panels that can generate electricity from sunlight on both their front and back sides. Unlike traditional monofacial solar panels, which are designed to only capture sunlight from one side, bifacial modules are designed to capture sunlight from both the front and the back, increasing their overall efficiency and power output. The increase in efficiency is achieved by the use of transparent backsheets and the reflection of sunlight from the ground or other surfaces onto the

back side of the panel. Bifacial modules are often used in large-scale solar projects and are well-suited to environments with high levels of diffuse radiation, such as cloudy or overcast conditions. However, they are also more expensive than traditional monofacial panels, so the increased efficiency must be weighed against the higher cost.

These panels are designed to capture light from both the front and the back, increasing their overall efficiency and power output. Bifacial modules use transparent backsheets to allow light to reach the back side of the panel, which can then be reflected from the ground or other surfaces to generate additional electricity. This makes them well-suited for large-scale solar projects and environments with high levels of diffuse radiation, such as cloudy or overcast conditions. However, bifacial modules are often more expensive than traditional monofacial solar panels, so the increased efficiency must be weighed against the higher cost.

The tilt angle of bifacial solar panels is a critical factor that affects their power output and efficiency. The optimal tilt angle for bifacial solar panels depends on several factors, including the geographic location, the time of year, and the orientation of the panels. The optimal tilt angle for bifacial solar panels depends on several factors, including the location, climate, and the intended use of the panels. In general, a tilt angle that is close to the latitude of the location is recommended, as this will maximize the amount of solar radiation that the panels receive throughout the year.

In general, a tilt angle that is equal to the latitude of the installation location is considered optimal for maximizing the power output of bifacial solar panels. For example, if the installation is located at a latitude of 35°, a tilt angle of 35° would be optimal. However, this may not always be the most practical or efficient solution, as the optimal tilt angle can vary depending on the specific circumstances of the installation. For example, in the Northern Hemisphere, a tilt angle of around latitude +15° is recommended, while in the Southern Hemisphere, a tilt angle of around latitude -15° is recommended. The tilt angle can be adjusted to optimize the panels for specific seasons or conditions, such as the winter solstice or the summer solstice. The tilt angle of bifacial solar panels can also be adjusted to optimize their performance throughout the year. For example, a steeper tilt angle may be used during the summer months to maximize power output, while a shallower tilt angle may be used during the winter months to reduce shading and maximize the amount of reflected light that reaches the back of the panels. It is important to note that the back side of bifacial solar panels is also exposed to light, so the panels must be installed

in a way that allows for unobstructed access to the light on both the front and the back. This may require additional considerations, such as shading from nearby buildings or trees, which can affect the performance of the panels. An experienced solar installer can provide guidance on the best tilt angle for a specific installation and help ensure that the panels are installed for optimal performance.

Ultimately, the best tilt angle for bifacial solar panels is one that provides a balance between maximum power output and minimized shading, taking into account the specific requirements of the installation and the local climate conditions.

Artificial intelligence (AI) can play an important role in the prediction of the optimal tilt angle for bifacial solar panels. By using machine learning algorithms, AI can analyze large amounts of data, including weather patterns, solar radiation levels, and energy consumption data, to identify patterns and make predictions about the performance of solar panels at different tilt angles. Artificial intelligence (AI) can play a significant role in predicting the optimal tilt angle for bifacial solar panels, as it can help to analyze large amounts of data and make accurate predictions based on complex patterns and relationships.

For example, AI can be used to predict the amount of solar radiation that a panel will receive at a given tilt angle, taking into account factors such as the location, time of year, and cloud cover. This information can be used to determine the optimal tilt angle for a specific installation. AI algorithms can be trained on historical weather data and satellite imagery to accurately predict the amount of diffuse radiation and direct sunlight that a specific location will receive throughout the year. This information can then be used to determine the best tilt angle for the panels to optimize their performance and maximize their power output.

In addition, AI can also be used to monitor the performance of solar panels in real-time, allowing for adjustments to be made to the tilt angle and other factors to optimize performance and increase energy efficiency. The use of AI in the prediction of the tilt angle of bifacial solar panels can help increase the overall efficiency and effectiveness of solar energy systems, reducing costs and increasing the amount of clean energy generated. The use of AI in predicting the tilt angle of bifacial solar panels can play a critical role in ensuring that the panels are installed and operated for optimal performance, and can help to maximize the investment in renewable energy

1.1   Background, Scope and Motivation

There is an increasing concern in recent times about the adverse effects of conventional energy sources on the environment. The utilization of fossil fuels like coal, oil, and gas has resulted in elevated levels of carbon emissions, which in turn are contributing to climate change. Climate change is a global issue that poses a threat to human health, the environment, and economic growth. The need to reduce carbon emissions and combat climate change has become a pressing issue for governments, businesses, and individuals worldwide.

The demand for energy continues to grow, driven by population growth, industrialization, and technological advancements. As the world becomes more urbanized and industrialized, the demand for energy will continue to rise. However, fossil fuels, which have been the primary source of energy for decades, are finite and limited in availability. The continued use of fossil fuels is unsustainable in the long term, and alternative sources of energy are needed to meet the growing demand for energy.

Renewable energy sources, such as solar, wind, and hydropower, offer a sustainable and diverse source of energy. Unlike fossil fuels, these sources of energy are not finite and do not contribute to carbon emissions. The need for a diverse and sustainable energy mix, including renewable energy sources, has become increasingly important as the world seeks to reduce carbon emissions and combat climate change.

One of the most promising developments in sustainable energy is the potential of net-zero energy buildings. These buildings are designed to generate as much energy as they consume, resulting in zero net energy consumption. The potential of net-zero energy buildings to contribute to a more sustainable future cannot be overstated. As the world becomes more urbanized and the demand for energy continues to grow, net-zero energy buildings offer a promising solution to the challenges posed by climate change and limited fossil fuel resources.

The environmental impact of traditional energy sources, the need to reduce carbon emissions and combat climate change, the growing demand for energy worldwide, the limited availability and finite nature of fossil fuels, the need for a diverse and sustainable energy mix, including renewable energy sources, and the potential of net-zero energy buildings to contribute to a more sustainable future are all critical issues that need to be addressed. It is essential that governments, businesses, and individuals work together to transition to a more sustainable

energy system that will meet the energy needs of the future while protecting the environment and promoting economic growth.

CHAPTER 2: LITERATURE REVIEW

As the global economy continues to expand rapidly, the supply and demand of energy have significant effects on social, economic, and environmental factors. Due to the necessity of achieving sustainable outcomes, policymakers have been obliged to set sustainable targets to steer economic policies in the direction of sustainability. This process is commonly known as the Sustainable Development Goals (SDGs), which were put forward by the United Nations. The energy sector is a crucial area with immense potential for advancements in technology and regulations. Solar energy is one of the most effective solutions suggested for reducing the economic and environmental impacts of energy use [1]. Rapid population growth and increasing living standards lead to a higher demand for energy across the world. However, traditional energy sources like fossil fuels are limited and have negative environmental impacts, such as greenhouse gas emissions, air pollution, and water pollution. Therefore, there is an urgent need to shift towards sustainable energy sources such as solar, wind, hydropower, geothermal, and biomass energy. These renewable energy sources are abundant, widely distributed, and do not release harmful emissions into the atmosphere. Moreover, renewable energy technologies have become more cost-effective and efficient over time, making them a viable alternative to fossil fuels [2].

Fossil fuels are finite resources and their use contributes significantly to greenhouse gas emissions and climate change [3]. The continued reliance on these fuels also poses risks to human health and the environment through air pollution, water pollution, and the risk of oil spills [4]. In contrast, renewable energy sources, such as solar, wind, hydro, geothermal, and biomass, offer clean and sustainable sources of energy that have the potential to mitigate these negative impacts [5]. Additionally, renewable energy technologies are becoming more cost-effective and are rapidly growing, making them a viable alternative to traditional fossil fuels [6].

For the past few decades, renewable energy has been widely recognized as a powerful remedy for the energy crisis [7]. Solar energy is considered one of the cleanest and most sustainable sources of energy among the available options, and it has the potential to significantly reduce or even eliminate carbon emissions [8]. Solar energy is a highly accessible and abundant source of renewable energy, as it is available in most parts of the world. In fact, in just 90 minutes, the earth receives enough solar energy from the sun to meet the world's energy

needs for an entire year. Additionally, the amount of solar energy that reaches the earth is 4200 times greater than the projected global energy demand for the year 2035 [9]. Solar energy systems that are intelligent and have a high capacity for collecting solar energy hold the promise of fulfilling the world's energy requirements without relying on any other energy sources [10]. Compared to fossil fuels, solar energy offers substantial environmental advantages since the carbon emissions during the lifecycle of solar panels are 95% lower than those of coal [11].

Table 1: Nomenclature

Nomenclature	
LSTM	Long Short-Term Memory
RNN	Recurrent Neural Network
CNN	Relative Humidity
BP	Barometric Pressure
WD	Wind direction
WS	Wind Speed
PV	Photo-Voltaic
RH	Relative Humidity
T_{air}	Ambient Air Temperature
R2	Coefficient of Determination
MAE	Mean Absolute Error
MSE	Mean Squared Error
RMSE	Root Mean Squared Error
BO	Bayesian optimization

Moreover, the Photovoltaic system has demonstrated a significant advantage over other energy sources, as it produces virtually no carbon emissions. Despite the enormous potential of solar energy to meet the world's energy needs, it currently accounts for a small fraction of the world's overall energy mix [12]. Likewise, Previous research suggests that solar photovoltaic technology can effectively utilize the power of the sun to produce environment friendly electricity on a large scale using local resources [13]. The production of electricity through solar energy is considered a renewable alternative to non-renewable technologies. Hence, it is fair to assert that the implementation of solar energy is eco-friendly compared to any other energy source and promotes the conservation of natural resources [14]. In addition, there have been efforts to forecast the potential of Solar Hydrogen production in the Islamabad region of Pakistan using Machine Learning methods. To accomplish this task, the Photovoltaic-Electrolytic (PV-E) system was selected to predict both electricity and hydrogen production [15].

The rapid increase in population and urbanization is driving up energy demands as shown in figure 1. Building electricity consumption accounts for around 40% of global energy consumption, as per the International Energy Agency's Energy Statistics 2019. Numerous countries have taken steps to tackle this issue by enacting policies and regulations that aim to enhance the energy efficiency of buildings and encourage the adoption of renewable energy sources (RES) to attain Zero-energy buildings. Net Zero Energy (NZE) buildings, which are both energy-efficient and sustainable, produce renewable energy on-site to meet or surpass the building's yearly local energy consumption. Solar energy is one of the most popular RES due to its widespread availability [16]. However, solar PV panels can be unreliable due to non-uniformity of irradiance and climate conditions. Bifacial PV panels have gained attention due to their complementary nature.
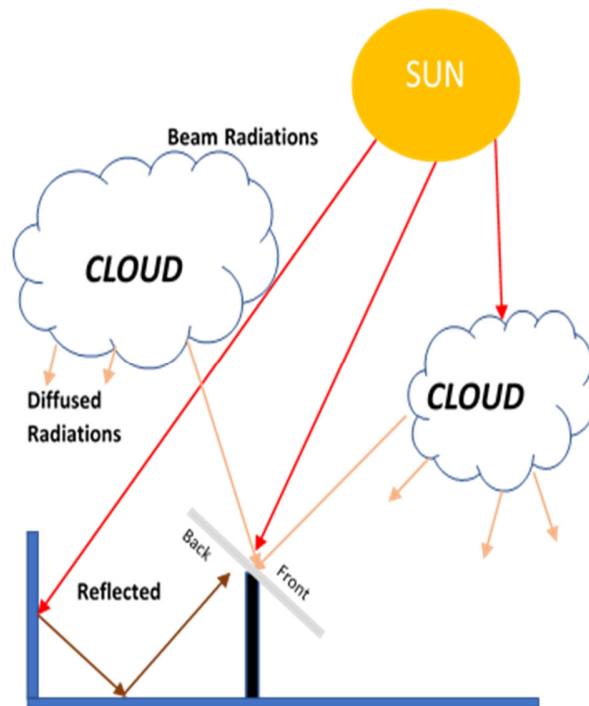
Figure 5: Bifacial Photovoltaic panels representation

Bifacial solar modules have the ability to collect sunlight from both sides, resulting in higher energy generation within the same surface area as monoracial modules as shown in figure 5. This makes bifacial technology an attractive option for the solar photovoltaic (PV) industry. A recent analysis conducted by Guerrero-Lemus and colleagues provides an overview of the evolution of bifacial technology from its early stages in the 1960s to its current practical applications and scalability. Despite the potential for increased energy output with the same

footprint, the widespread deployment of bifacial PV technology had to wait for recent advancements in technology [17].

Commercial PV cells are typically rated to have an efficiency range between 10% to 20%, with an associated cost of \$0.1-0.24 per kilowatt-hour. However, the remaining solar energy that is not converted to electricity is mostly dissipated as heat, leading to a decrease in the voltage generated and therefore a decrease in the overall efficiency of the cell [18]. Furthermore, shading losses can occur in a solar panel when shaded cells force every cell in the panel to operate at a reduced current. This issue can be resolved by placing the panels on the roof or in open lots [19]. On the other hand, it is possible to enhance the total energy output of solar panels. Bifacial solar module technology is a promising emerging trend in rooftop PV systems for energy generation, which is expected to dominate PV installations in the near future due to its technological and economic feasibility [20]. Optimal planning strategy for distributed rooftop photovoltaic systems in high-density cities using integer learning programming and high-accuracy solar energy potentials characterization was proposed [21]. It has been reported that highly reflective and light-colored surfaces can enhance the energy output of bifacial solar panels by 10% to 30% [22].

To further improve the energy harvesting efficiency, an effective Maximum Power Point Tracking (MPPT) algorithm such as learning-based real-time hybrid global search adaptive approach can be employed this approach can lead to even greater energy extraction efficiency [23]. Photovoltaic Maximum Power Point Tracking also been done by Artificial Neural Networks [24]. A set of empirical design rules was developed to evaluate the efficiency of bifacial modules in various regions worldwide. These rules are designed to optimize bifacial solar modules and enable rapid assessment of location-specific performance. It was also concluded that for actual installation, detailed local meteorological data is essential, whereas the NASA satellite-derived insolation database is only suitable for preliminary estimation [25]. A coupled optical-electrical-thermal model of bifacial solar panels was introduced, utilizing a solarGIS database to acquire Global Horizontal Irradiance (GHI) and Diffuse Horizontal Irradiance (DHI) data [26]. The prediction of short- and long-term solar irradiance using deep learning algorithms has been the focus of research conducted by Haider et al., while various studies have also investigated ways to evaluate and improve the performance of solar panels, including the development of different types of solar simulators [27]. A solar simulator was

designed by utilizing a 1,000 W metal halide lamp coupled with a truncated ellipsoidal reflector optimized through parametric iterations, as reported by Shah et al. (2020) [28]. When evaluating solar load using bifacial solar panels in a humid sub-tropical region during the monsoon season, on-site data from mid-June to mid-August was utilized as an input for solar ray tracing. Due to the large temperature variations and extended cloud cover, the effect of changing weather patterns was observed. A comparative analysis of the SOPLOS and ASHRAE models with the in-situ model was conducted, revealing that both models overestimate front side solar load, with only 0.5% and 13% of their estimations aligning with in situ data respectively. In contrast, both models underestimate rear side solar load during the studied time period, with only 2% and 24% of their estimations matching with in situ data respectively [29].

In recent years, there has been a significant increase in the development of solar modelling and ray tracing tools, which has led to a more accurate and reliable assessment of solar energy potential. These tools utilize various algorithms and techniques, like acceleration strategies were utilized to reduce heavy ray tracing requirements by almost 90% for modeling bifacial illumination of full photovoltaic systems annually using ray tracing, as reported in a study [30]. In 2020, an open-source python toolkit named bifacial radiance was created to automate the performance assessment of PV systems within the ray tracing software tool RADIANCE [31], these techniques provide detailed information on solar irradiance, panel performance, and energy yield. Other researchers have also explored the concept of net-zero energy solar greenhouses (NZESGs), such as a study that investigated the potential for integrating vertical bifacial photovoltaic panels into a greenhouse structure to achieve near-zero energy consumption in tomato production. Another study proposed a design for an NZESG that utilizes a solar wall and earth-tube heat exchanger system to improve energy efficiency and reduce heating costs [32]. Despite the availability of these tools, there remains a clear research gap in terms of experiment validation. Many of these tools lack real-world validation, which means that their accuracy and reliability have not been fully tested in practice. Without proper validation, there is a risk of inaccurate predictions and unreliable assessments, which could result in significant financial losses for solar energy projects. Therefore, there is a pressing need for more research to validate the accuracy and reliability of these tools in real-world conditions.

The focus of this study is to gather data through experimentation on solar bifacial panels. Specifically, the study will collect data on the half-hourly front-side radiative flux (q_r) and its

variation in relation to both the tilt angle of the panels and the prevailing weather conditions. This research is significant because it can provide insights into how solar bifacial panels perform under different circumstances, and it can help to optimize their performance in real-world applications. The data collected in this study can also inform future research and development in the field of solar energy, which is becoming increasingly important as the world seeks to transition to more sustainable forms of energy production. The collected data on the half-hourly front-side radiative flux (q_r) and its variation in relation to the tilt angle and weather conditions can also be used to develop machine learning models that can predict the optimum tilt angle for solar bifacial panels. By using this data to train a machine learning algorithm, the algorithm can learn the patterns and relationships that exist between the tilt angle, weather conditions, and radiative flux, and then use this information to predict the optimal tilt angle for a given set of conditions. This approach has the potential to improve the accuracy and efficiency of optimizing the tilt angle for solar bifacial panels, which can lead to more effective use of solar energy and greater energy savings. Furthermore, by integrating machine learning models into solar energy systems, it can be possible to develop more intelligent and autonomous solar energy systems that can optimize their performance in real-time based on changing environmental conditions.

CHAPTER 3: METHODOLOGY

An unsteady flow varies in time as either random or periodic manner The aim is to gather data through experimentation on solar bifacial panels, specifically focusing on the half-hourly front-side radiative flux and its relationship to the tilt angle of the panels and prevailing weather conditions. The collected data can also be used to develop machine learning models that can predict the optimum tilt angle for solar bifacial panels. By using this data to train an algorithm, the model can learn patterns and relationships between the tilt angle, weather conditions, and radiative flux. This approach can improve the accuracy and efficiency of optimizing the tilt angle for solar bifacial panels, leading to more effective use of solar energy and greater energy savings. Furthermore, integrating machine learning models into solar energy systems can develop more intelligent and autonomous systems that optimize their performance based on changing environmental conditions in real-time.
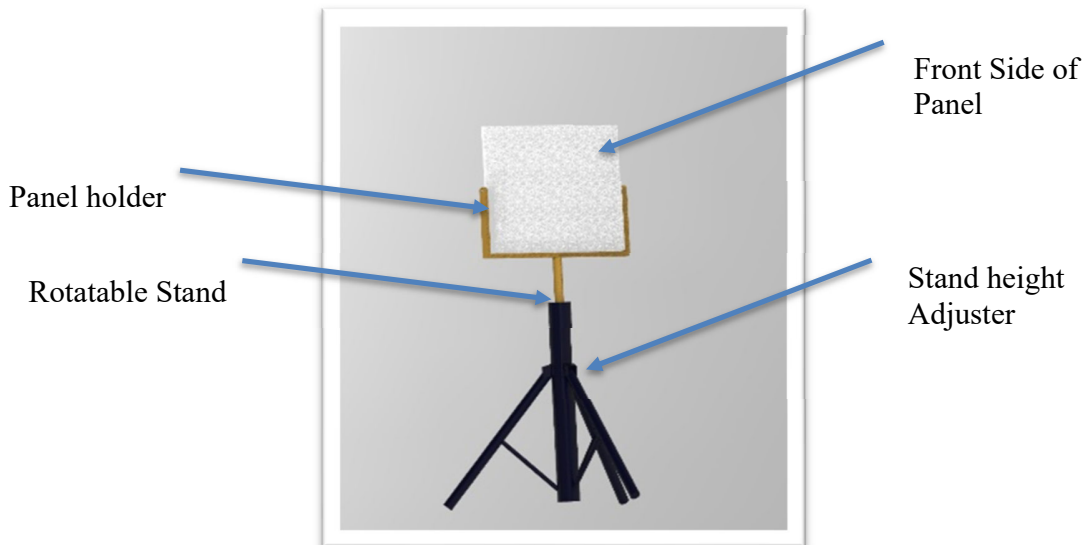
Figure 6: Computer Aided Design model

3.1 Experimental Setup

In our study, we aimed to collect data for forecasting bifacial solar panel irradiance based on climate parameters and tilt angle. To achieve this, we employed a data collection plan that involved the use of various sensors commonly used in weather stations to collect data on temperature, relative humidity, pressure, and wind speed. However, for irradiance data, we developed a prototype using a two-axis rotation system. This system allowed us to measure the

irradiance at different tilt angles and sun-facing angles, which we recorded alongside the other climate parameters. By using this innovative approach, we were able to collect more accurate and detailed data on irradiance, which is a critical factor in forecasting solar panel performance. This data can be used to develop more accurate models for forecasting solar panel irradiance, ultimately contributing to the development of more efficient and effective solar energy systems.
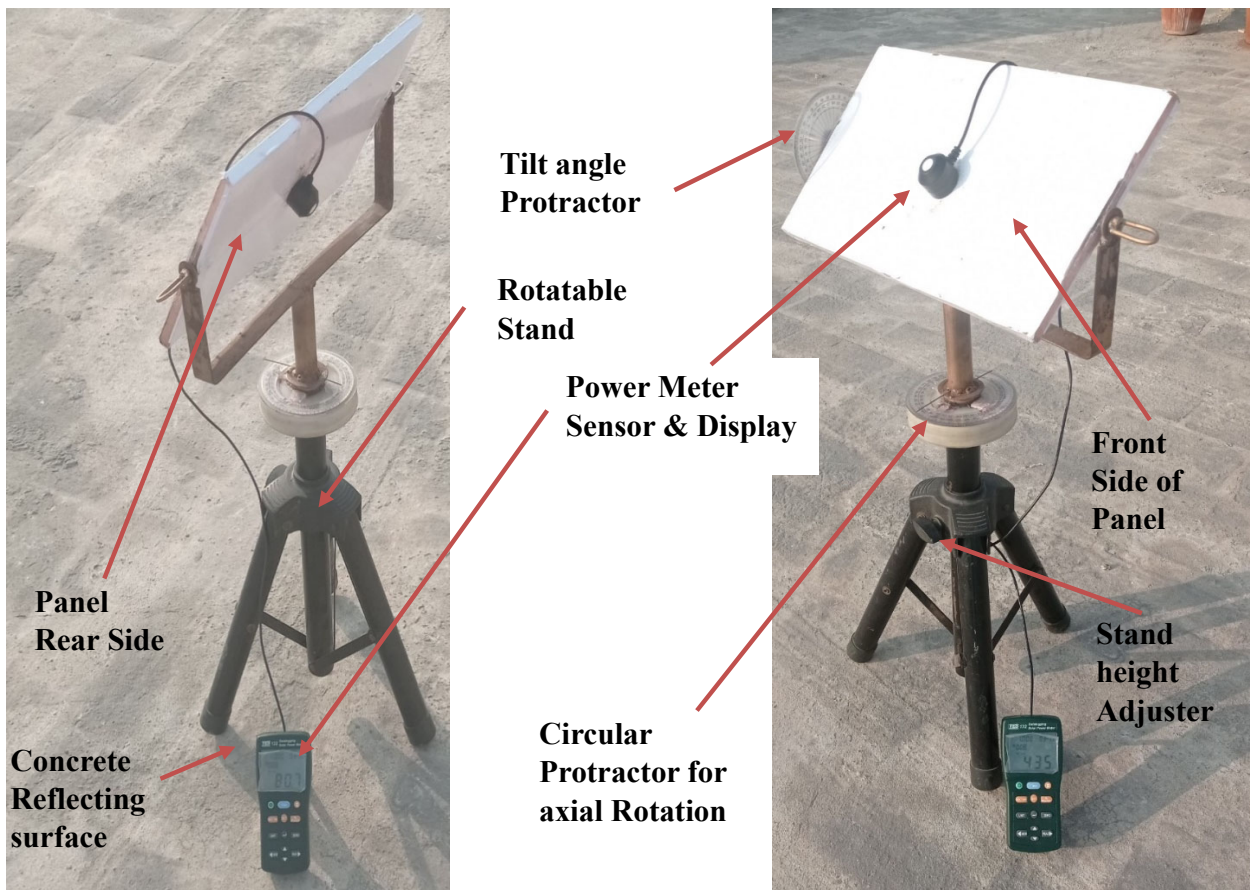
Figure 7: Demonstration of experimental setup

components, including a Circular Protractor for axial Rotation, a Protractor for Tilt angle, a Rotatable Stand, a Stand Height Adjuster, and a Concrete Reflecting surface as shown in figure 3. These parts were carefully selected to provide a flexible and reliable platform for measuring irradiance data at different tilt angles and sun-facing angles. To record the half-hourly radiative flux data, we also attached a solar power meter to the prototype. This device allowed us to accurately measure the electrical output of the solar panel and record the irradiance data at

regular intervals. The Rotatable Stand allowed us to rotate the solar panel along its horizontal axis, while the Stand Height Adjuster enabled us to adjust the height of the stand to suit different measurement scenarios. Both the Circular Protractor and the tilt angle Protractor were used to measure the tilt angle and sun-facing angle of the solar panel. These angles were critical in determining the irradiance on the bifacial solar panel.

Table 2: Details of Experiments.

Time	Environmental parameters	Sun Facing Angle Ø	Tilt Angle β	Side
t0	e0	Ø0	β0	s0
t1	e1	Ø1	β1	s1
t2	e2	Ø2	β2	
t3	e3	Ø3	β3	
t4	e4	Ø4	β4	
t5	e5	Ø5	β5	
t6	e6	Ø6	β6	
t7	e7	Ø7		
t8	e8	Ø8		
t9	e9	Ø9		
t10	e10	Ø10		
t11	e11	Ø11		
t12	e12	Ø12		
t13	e13	Ø13		
t14	e14	Ø14		

3.2 **Process flow:**

Due to the urban environment where the experimentation was conducted and in support of the zero-energy building concept, we used a Concrete Reflecting surface to reflect sunlight back onto the solar panel during measurement. This surface helped to maximize the amount of available sunlight for the solar panel, thereby increasing the accuracy of the irradiance measurements. By using this prototype, we were able to collect precise and reliable data on irradiance in an urban environment, which is essential for forecasting solar panel performance in such settings. This data can be used to develop more accurate models for forecasting solar panel

irradiance in urban areas, ultimately contributing to the development of more efficient and effective solar energy systems for zero energy buildings.

3.3 Data set collection:

In this study, we used a variety of sensors to collect data on the different climate parameters that may impact bifacial solar panel performance. The sensors we used, along with their corresponding variables, descriptions, instruments, and accuracy, are presented in the table 3.

Table 3: Details of Instruments.

Variable	DESCRIPTION	Instrument	Range & Accuracy
I	Irradiance	Solar Power Meter TES 132	±10 W/m² at 25°C
T_{air}	Air Temperature	Campbell CS215	±0.3 °C at 25 °C
RH	Relative Humidity	Campbell CS215	@ $25C^o$, ±2%
WS	Wind Speed in m/s	NRG 40H Anemometer	0.2 m/s range 6 m/s to 25 m/s
WS_Max	WS maximum within the time interval	NRG 40H Anemometer	0.2 m/s range 6 m/s to 25 m/s
WD	Wind direction in ∘N (to East)	NRG 200 Wind Direction Sensor	±1.6° and dead band region is ±4.3°
WS_std	Wind Standard Deviation	Na	Na
BP	Barometric Pressure	Campbell CS100 Barometric Pressure Sensor	±0.5 hPa 20°C

The meteorological data was collected for a duration of four weeks, covering two weeks before and after the winter solstice. The measurements were taken at half-hour intervals using accurate meteorological instruments, which were placed in the EMAP Tier 1 Meteorological station located in Islamabad at coordinates 33.64∘N 72.98∘E, and an altitude of 500 meters above

sea level. The experimental setup used to collect the data is illustrated in Figure 1, while Table 3 provides a comprehensive description of the variables in the dataset and the corresponding instruments used for their recording.

The irradiance values of cloudy days are absorbed to be relatively low, indicating the impact of weather conditions on the performance of bifacial solar panels. we observed that the effect of weather conditions is more significant on the front side of the solar panel than on the back side. This finding is consistent with previous studies on bifacial solar panels. Furthermore, the selection of dates for experiments before and after winter solstice allowed us to capture the variation in weather conditions over time. The collected data and the observed patterns will help us in developing an accurate forecasting model for irradiance values based on climate parameters and tilt angle, which is crucial for the optimal operation of bifacial solar panels.

3.4 **Data Representation:**

By using the above-described sensors, we were able to collect highly accurate and precise data on the climate parameters affecting the performance of bifacial solar panels. This data will enable us to better understand how solar panel performance is influenced by these parameters and ultimately improve the forecasting of solar irradiance. In the experimentation section, we collected time-series data that included several parameters such as air temperature, relative humidity, barometric pressure, wind speed, sun-facing angle, tilt angle, radiation on the front of the solar panel, radiation on the back of the solar panel, the ratio of back to front radiation, and the total radiations. These data were collected at half-hourly intervals using the sensors mentioned earlier. The data were recorded with a time step and the values for each parameter were noted accordingly. The data were collected over a period of time and recorded in a table with columns for each parameter. The datetime column contained the time at which the data were recorded. The remaining columns contained the values for air temperature, relative humidity, barometric pressure, wind speed, sun-facing angle, tilt angle, wind direction, wind speed standard deviation, wind speed maximum   and the total radiations

Table 4: Data Description

SR No:	Date Time	Air Temperature (C^o)	Relative Humidity (%)	Pressure (mbar)	Wind Speed m/s	Wind direction in °N (to East)	Wind speed Standard Deviation	Wind Speed maximum	Sun Facing Angle (°)	Tilt angle (°)	Radiations (W/m^2)
	Week 1										
1	07/12/2022 09:00	12.67	61.25	938.1916	1.375	96.8	0.031	1.375	0	90	906
...	...	...	...	...	...	...	...	...	...	...	...
100	07/12/2022 16:00	19.1	35.65	967.4251	6.905	268.8	15.51	6.905	115	45	586.7
...	...	...	...	...	...	...	...	...	...	...	...
110	08/12/2022 09:00	13.28	56.32	937.1371	0.749	28.47	0.002	0.749	0	45	1026
...	...	...	...	...	...	...	...	...	...	...	...
	Week 2										
930	15/12/2022 12:00	19.87	31.62	974.5694	4.643	265.6	23.95	4.643	42	90	1110
...	...	...	...	...	...	...	...	...	...	...	...
	Week 4										
2295	01/01/2023 13:30	17.33	35.76	965.2537	3.135	178.4	13.36	3.135	65	75	1256
...	...	...	...	...	...	...	...	...	...	...	...

In our study, we analyzed the relationship between solar irradiation and climate parameters using Python. The correlation plot in figure 4 illustrates the degree of correlation between each variable and solar irradiation. Based on the correlation plot, we observe a high dependency of solar irradiation on tilt angle, sun-facing angle, and relative humidity. This suggests that these variables play a significant role in predicting solar irradiation levels on bifacial solar panels. We can see that as tilt angle increase, solar irradiation also increases. Additionally, we see a negative correlation of relative humidity and sun-facing angle on solar

irradiation, indicating that higher relative humidity and sun-facing angle levels result in lower solar irradiation levels.
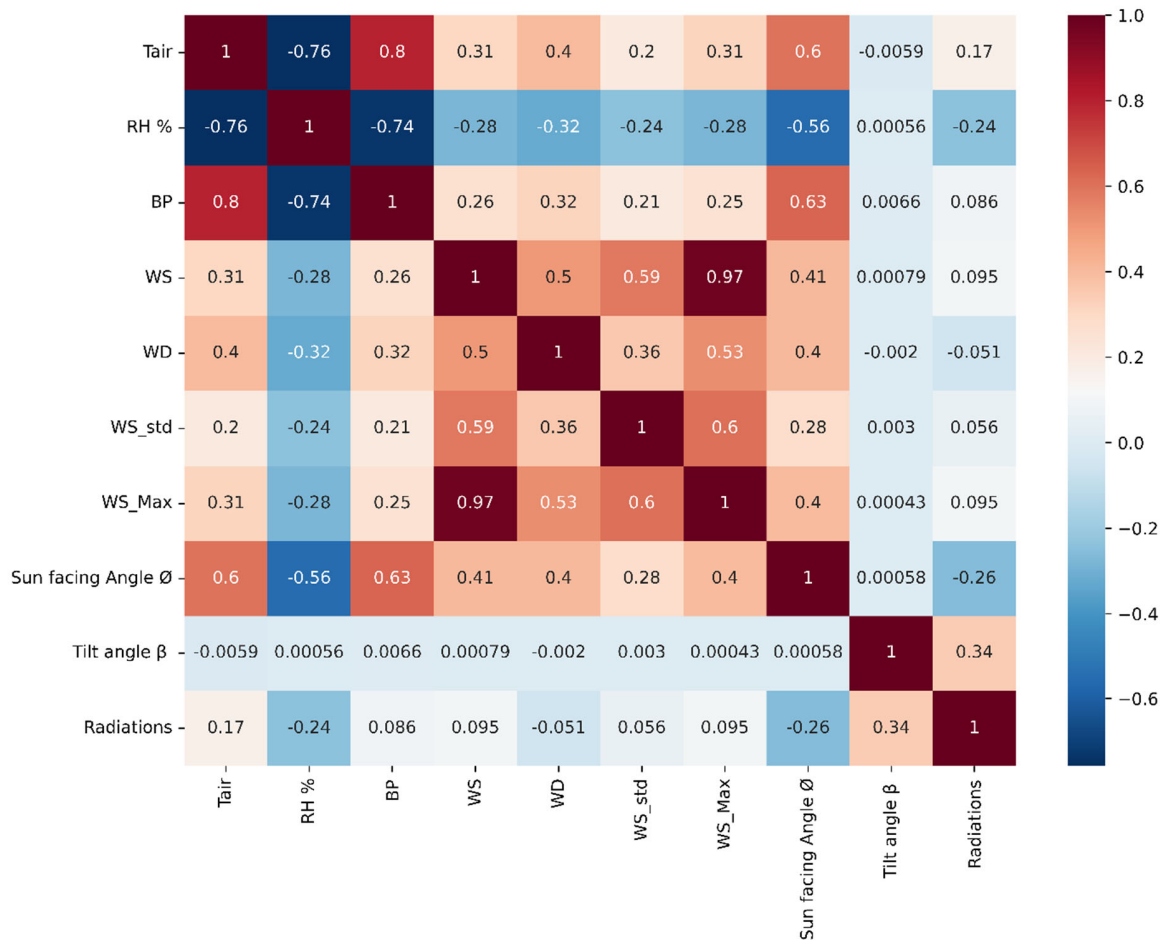

Figure 8. Correlation Plot of Features

On the other hand, the correlation between solar irradiation and wind speed and air temperature is relatively low. This implies that these variables may not be as significant in predicting solar irradiation levels on bifacial solar panels. The correlation plot provides valuable insights into the relationship between solar irradiation and climate parameters. These findings can be used to optimize the placement and positioning of bifacial solar panels to maximize their efficiency in different climates.

3.5 Data pre-processing:

To ensure data quality, all datasets are initially inspected for any anomalies before they are used to train or test the models. During exploratory data analysis, it was discovered that a significant number of solar irradiation readings were recorded as zero or extremely low, which can be attributed to rainy days. However, the presence of these values can interfere with model fitting, as it turns out that out of 3,234 total records, 442 solar irradiation values were equal to zero. To overcome this issue, all readings corresponding to rainy days were removed from the dataset, resulting in 2,792 valid records for further analysis.

3.6 Dataset distribution:

The dataset for Deep Learning methods was divided into three subsets, namely Training, Validation, and Test sets. The Training set consisted of 70% of the dataset, which corresponds to 1955 records. The Validation set included 15% of the total data, equivalent to 418 records, while the Test set also had 15% of the total data, which amounts to 418 records.

3.7 Forecasting Models:

Deep Learning is a powerful tool that can handle various types of data, whereas LSTM (Long Short-Term Memory) is a specialized type of network within Deep Learning that is designed for processing sequential and time-series data. Predicting solar irradiance is crucial for power system generation and planning. Traditional statistical methods like autoregressive moving average, support vector machine, and artificial neural network have limitations like low accuracy, scalability issues, and inability to capture long-term dependencies. To overcome these, a deep recurrent neural network is proposed and tested using real data from the National Resources in Canada, demonstrating improved accuracy and advantages over existing methods [33].

The flowchart for the deep learning algorithm used in this study is shown in figure 5. The first step in the process involves collecting the data, which was obtained from the experimentation. The data consists of solar irradiance values measured in watts per square meter (W/m2) at one-minute intervals. The data was then preprocessed, which included data cleaning and normalization. The cleaned data was then split into training, validation, and testing datasets, with 70% of the data used for training, and 15% each for testing and validation data. The training

dataset was used to train the RNN-LSTM and Transformers deep learning models. The hyperparameters for the models were optimized using Bayesian optimization, which involves selecting the best set of hyperparameters based on the results of the previous iterations.

After the models were trained, they were tested using the testing dataset to evaluate their performance. The performance of the models was measured using evaluation metrics. The models were then used to make predictions of solar irradiance values for a range of forecasting horizons, ranging from 10 minutes to 90 minutes into the future. The predictions were compared to the actual values using the evaluation metrics to assess the accuracy of the models. The flowchart shows the process of collecting and preprocessing the data, training the deep learning models using Bayesian optimization, testing the models using the testing dataset, and making predictions for different forecasting horizons. The use of Bayesian optimization to optimize the hyperparameters and the distribution of data into training, validation, and testing datasets helped to ensure the accuracy and reliability of the deep learning models in forecasting solar irradiance values.
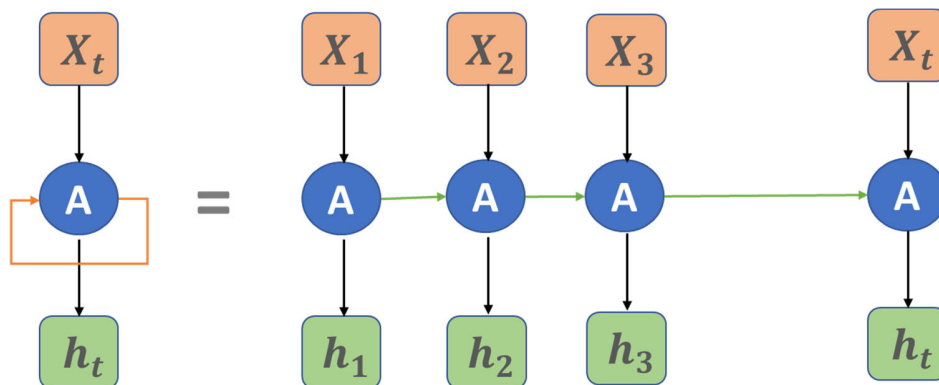

Figure 9. Unrolled recurrent neural network.

3.7.1 **RNN-LSTM:**

Recurrent Neural Networks (RNNs) have been widely used in various fields for sequential data analysis, such as speech recognition, natural language processing, and time-series prediction. However, standard RNNs suffer from vanishing gradient problem which makes it difficult to capture long-term dependencies in the input sequences. Long Short-Term Memory (LSTM) is a type of RNN architecture that addresses this issue by introducing memory cells,

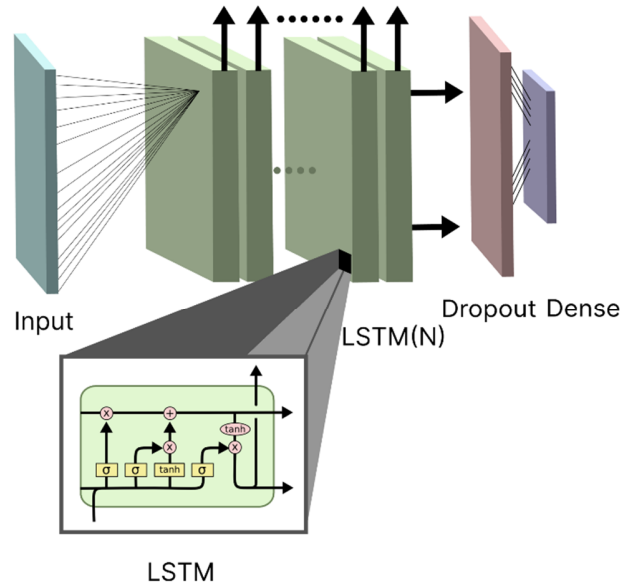which allow information to be stored for long periods of time without being diluted or lost shown in figure 7.

Figure 10. RNN-LSTM Architecture example.

LSTM has proven to be a powerful tool for time-series forecasting and has been applied in various fields such as energy, finance, and weather forecasting. For instance, in a recent study, LSTM was used to forecast photovoltaic power output based on meteorological data, achieving high accuracy compared to traditional models. Another study utilized LSTM to forecast wind turbine power output, showing improved accuracy compared to other machine learning models [34]. LSTM models have been utilized in numerous studies for time-series forecasting, such as predicting solar power output, wind power generation, and energy demand. In recent years, with the advancement of deep learning and big data technologies, LSTM models have been further improved and optimized to achieve better performance in various applications.

3.7.2 **Transformers**

The Transformer model is a sequence-to-sequence architecture that can encode and decode input data to produce an output sequence [35]. To forecast Solar Irradiance, a four-block Transformer architecture with eight heads of size 256 is used, along with a position encoding layer to capture temporal patterns and dependencies in the input sequence. Multiple transformer

blocks, each with eight transformer heads, are used, and the output of the positional encoder is directed to them. Two 1d convolution layers with kernel sizes of 1 and filter sizes of 8 and 74 (corresponding to the number of features in the dataset) are implemented in the feedforward layer. A dense layer with 256 units generates the final output after the output data passes through multiple transformer blocks. The Transformer model's self-attention mechanism, which allows the network to weigh input components when making predictions, is a defining characteristic [36]. This feature enables the Transformer to process input of varying lengths, unlike traditional RNNs, which are limited by a fixed-length context [37]. Additionally, the Transformer model's multi-head attention mechanism allows it to handle data from different representation subspaces at distinct positions.

3.7.3 Bayesian Optimization:

Bayesian optimization is a powerful optimization technique that is commonly used in machine learning algorithms such as Recurrent Neural Networks (RNNs) and Transformers. It is an approach that involves iteratively constructing a probabilistic model of the objective function and using it to select the next query point, which is then evaluated to update the model. The goal of Bayesian optimization is to find the global optimum of a function with a minimal number of evaluations.

The novelty of Bayesian optimization lies in its ability to efficiently explore high-dimensional search spaces with limited data. It employs a probabilistic model to capture the structure of the search space and uses it to guide the search towards promising regions of the space. Bayesian optimization has been shown to be effective in various applications, such as hyperparameter tuning and architecture search [38].
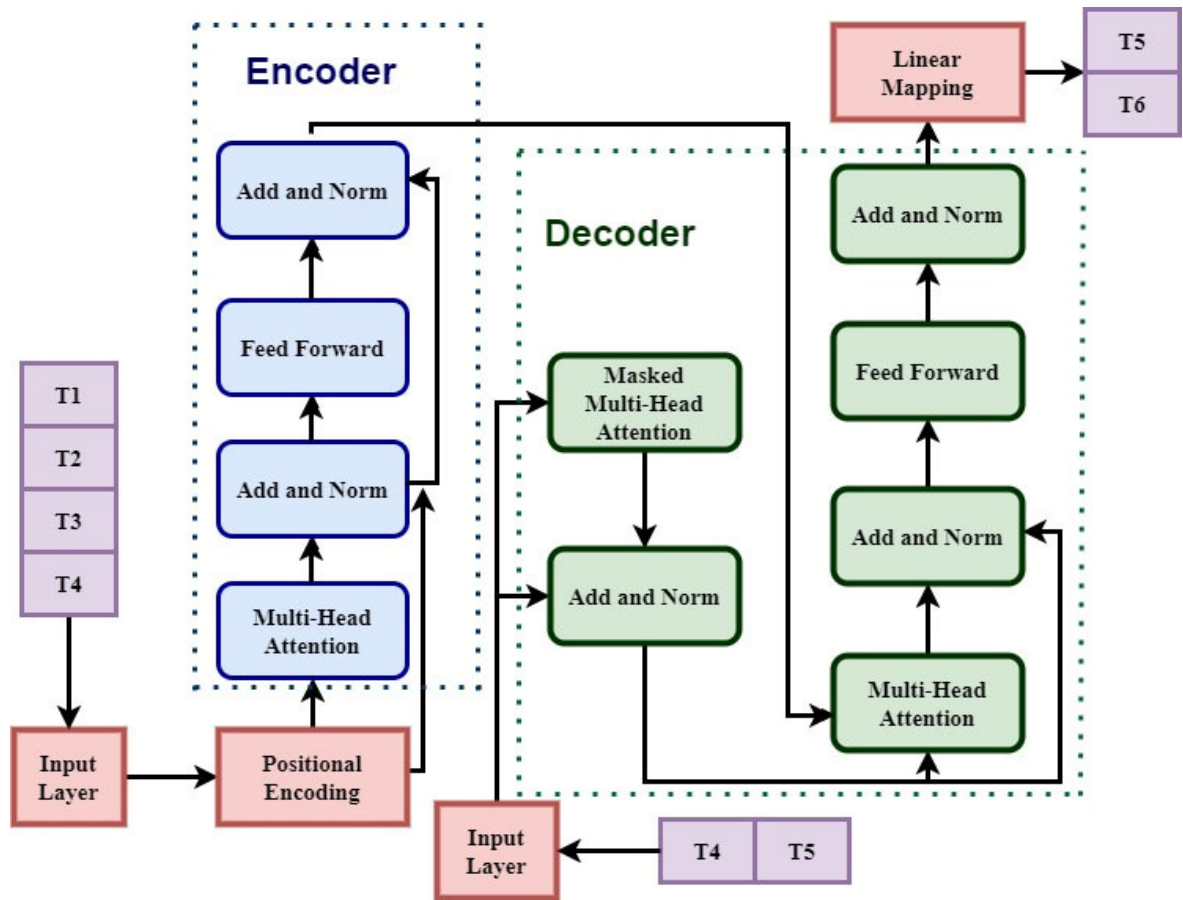
Figure 11: Architecture diagram of transformer neural network representing the flow of input sequences through multiple layers.

In the context of RNNs and Transformers, Bayesian optimization can be used to optimize hyperparameters such as learning rates, dropout rates, and the number of layers. This approach can significantly improve the performance of these models and reduce the time required for hyperparameter tuning. Additionally, Bayesian optimization can be combined with other optimization techniques such as gradient descent to further improve the optimization process. Overall, Bayesian optimization is a powerful and novel approach that can significantly enhance the performance of machine learning algorithms such as RNNs and Transformers.
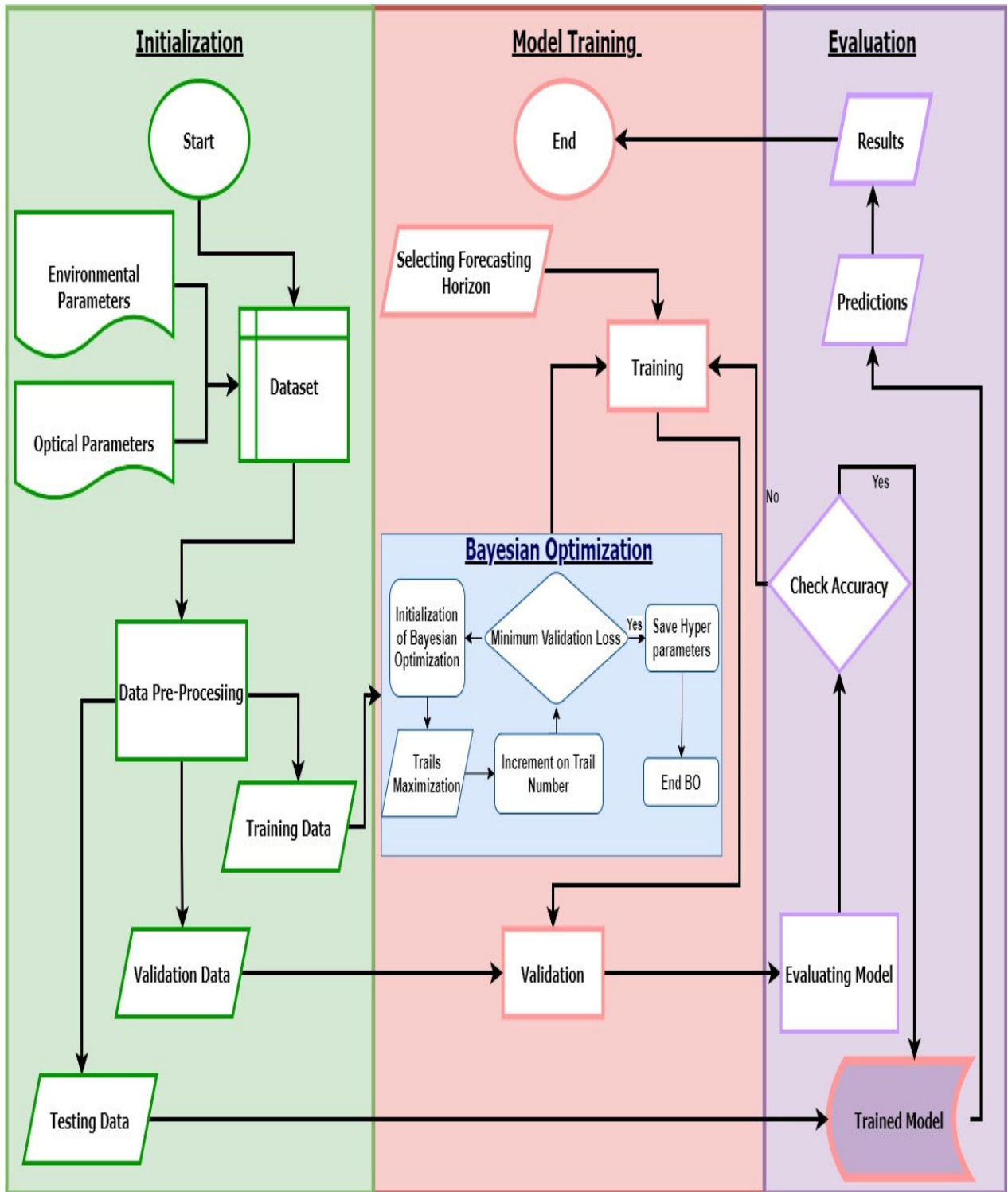
Figure 12. Complete process diagram

CHAPTER 4: RESULTS AND DISCUSSION

4.1 Evaluation Metrics:

The evaluation of machine learning models is a crucial aspect of data science, and matrixes have been developed to facilitate this process. To evaluate the performance of regression models, several matrixes are commonly used, including MAE, RMSE, SMAPE, and R2. MAE measures the average absolute difference between the actual and predicted values, making it easy to interpret and robust to outliers. However, it doesn't indicate the direction of the error. RMSE, on the other hand, gives more weight to large errors, making it more sensitive to outliers than MAE. However, it is harder to interpret and compare between models. SMAPE is useful when the magnitude of errors is critical, and it is less sensitive to outliers. R2 measures the proportion of the variance in the dependent variable that is predictable from the independent variable, and it is widely used to evaluate regression models. The range of R2 is from 0 to 1, where 0 indicates no variation in the dependent variable explained by the model, and 1 indicates complete explanation. As machine learning evaluation techniques continue to evolve, it is crucial to select the appropriate evaluation metrics based on the problem statement and the data type.

4.2 Model Evaluation:

Different evaluation metrics were employed to assess the effectiveness of RNN-LSTM and transformers deep learning models in predicting irradiations across different forecasting horizons. The findings from the study indicated that both models were effective in forecasting irradiations at different horizons. However, the transformers model outperformed the RNN-LSTM model as shown in Table 2 with lower Mean Absolute Error (MAE) values ranging from 0.05 to 0.03 across the same horizons. In contrast, the Transformers model had a MAE ranging from 0.03 at a horizon of 10 minutes to 0.11 at a horizon of 90 minutes. The difference in MAE values between the two models implies that the RNN-LSTM model has a higher accuracy in forecasting irradiations compared to the transformers model.

Table 5 : Comparison of performance between RNN-LSTM and Transformers at multiple Forecasting Horizons.

Evaluation Metrics	Forecasting Horizon	RNN-LSTM	Transformers
MAE	10 minutes	0.05	0.03
	30 minutes	0.07	0.06
	60 minutes	0.10	0.10
	90 minutes	0.13	0.11
RMSE	10 minutes	0.07	0.09
	30 minutes	0.11	0.12
	60 minutes	0.14	0.14
	90 minutes	0.18	0.15
SMAPE	10 minutes	7.326	10.348
	30 minutes	10.8265	14.41
	60 minutes	13.62	14.041
	90 minutes	17.00	18.011
R2	10 minutes	**0.927**	**0.894**
	30 minutes	**0.786**	**0.758**
	60 minutes	0.692	0.710
	90 minutes	0.48	0.64

The table provided shows the evaluation metrics for forecasting solar panel irradiance using two different deep learning models: RNN-LSTM and Transformers. The evaluation metrics used were MAE, RMSE, SMAPE, and R2. These metrics are commonly used to assess the accuracy and performance of forecasting models. In terms of MAE, both models performed similarly for shorter forecasting horizons of 10 and 30 minutes, with RNN-LSTM having slightly lower MAE values. However, as the forecasting horizon increased to 60 and 90 minutes, both models showed an increase in MAE, with Transformers having slightly higher MAE values than RNN-LSTM.

The RMSE metric also showed a similar trend, with both models having lower values for shorter forecasting horizons of 10 and 30 minutes, and higher values for longer forecasting horizons of 60 and 90 minutes. Again, RNN-LSTM had slightly lower RMSE values than Transformers for shorter forecasting horizons, while Transformers had slightly higher RMSE values than RNN-

LSTM for longer forecasting horizons. The SMAPE metric, which measures the relative percentage difference between the actual and predicted values, showed that both models had higher SMAPE values for longer forecasting horizons. However, Transformers had higher SMAPE values than RNN-LSTM for all forecasting horizons, indicating that RNN-LSTM performed better in terms of relative percentage difference.

Finally, the R2 metric, which measures the goodness of fit of the model, showed that RNN-LSTM had higher R2 values than Transformers for shorter forecasting horizons of 10 and 30 minutes. However, as the forecasting horizon increased to 60 and 90 minutes, Transformers showed higher R2 values than RNN-LSTM. Overall, the results suggest that both RNN-LSTM and Transformers are capable of accurately forecasting solar panel irradiance, with RNN-LSTM having a slight advantage for shorter forecasting horizons, and Transformers having a slight advantage for longer forecasting horizons. The choice of model may ultimately depend on the specific needs and requirements of the forecasting application.

RNN Training Graph with Forecasting Horizon 21 (No of Epoch Vs Validation Loss):

RNN Training graph With Forecasting Horizon 21": This graph shows the validation loss of an RNN model trained to predict a 21step forecasting horizon. The x-axis represents the number of epochs during training, while the y-axis represents the validation loss. The validation loss starts high and gradually decreases with each epoch until it stabilizes at around 50 epochs.
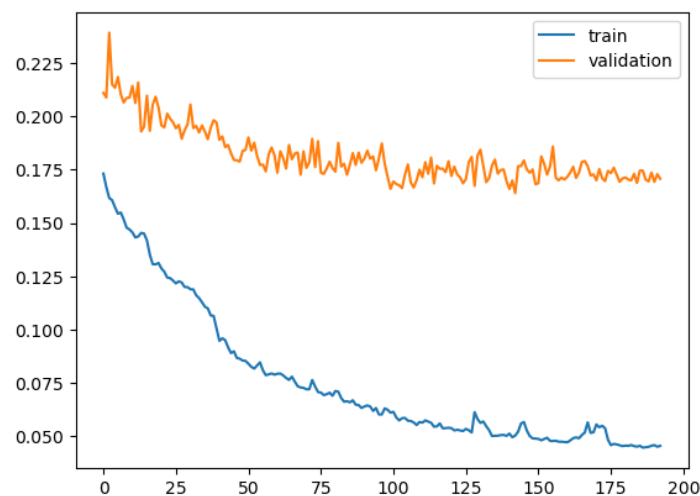

Figure 13. RNN Training Graph with Forecasting Horizon 21 (No of Epoch Vs Validation Loss)

Transformers Training Graph with Forecasting Horizon 21 (No of Epoch Vs Validation Loss):

TRANSFORMERS Training graph With Forecasting Horizon 21": This graph shows the validation loss of a Transformers model trained to predict a 21-step forecasting horizon. The x-axis represents the number of epochs during training, while the y-axis represents the validation loss. The validation loss starts high and gradually decreases with each epoch until it stabilizes at around 50 epochs, similar to the RNN model.
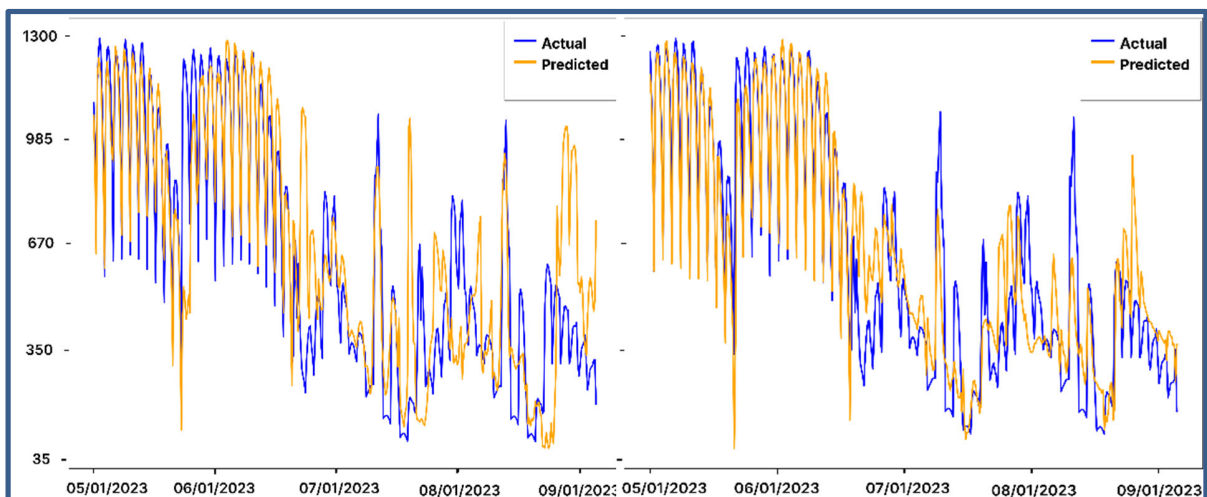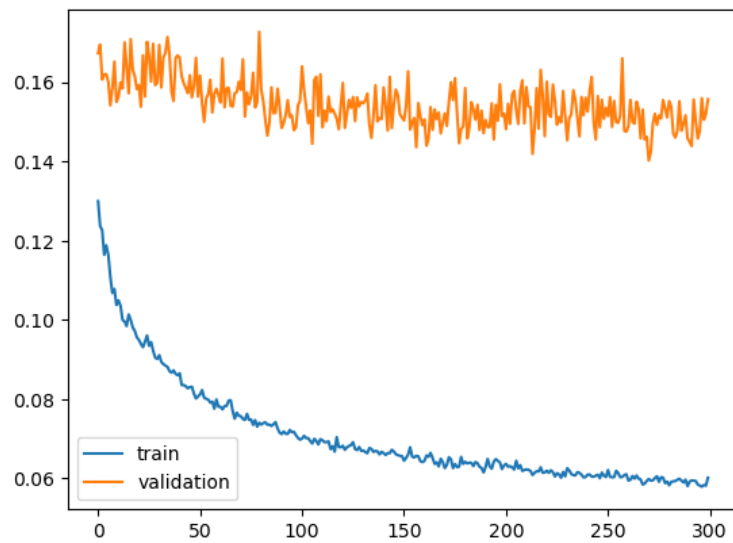

Figure 14. Transformers Training (a) and Validation (b) Graph with Forecasting Horizon 21 (No of Epoch Vs Validation Loss)

RNN Training Graph with Forecasting Horizon 14 (No of Epoch Vs Validation Loss):

RNN Training graph With Forecasting Horizon 14": This graph shows the validation loss of an RNN model trained to predict a 14-step forecasting horizon. The x-axis represents the number of epochs during training, while the y-axis represents the validation loss. The validation loss starts high and gradually decreases with each epoch until it stabilizes at around 50 epochs, but with a slightly lower final loss compared to the previous graph.
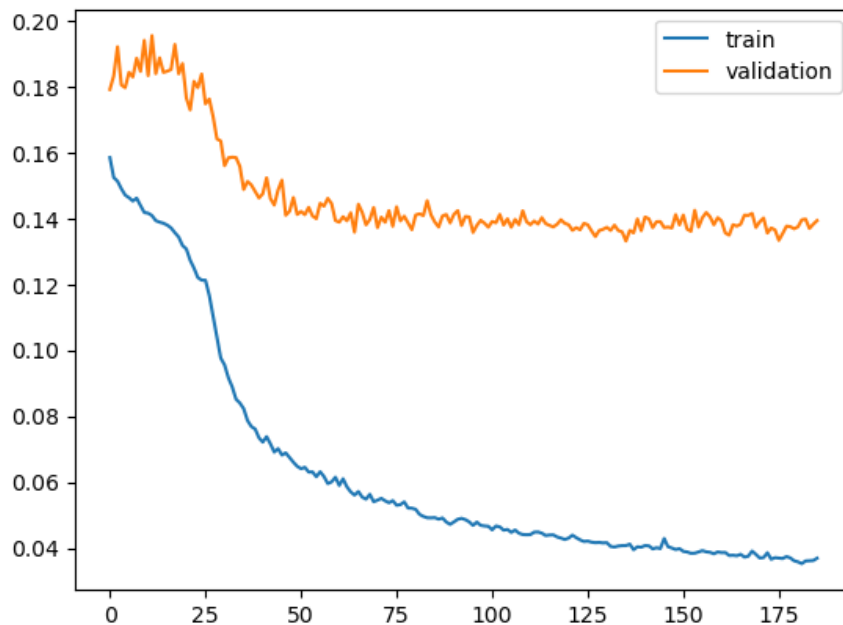

Figure 15. RNN Training Graph with Forecasting Horizon 14 (No of Epoch Vs Validation Loss)

Transformers Training Graph with Forecasting Horizon 14 (No of Epoch Vs Validation Loss):

TRANSFORMERS Training graph With Forecasting Horizon 14": This graph shows the validation loss of a Transformers model trained to predict a 14-step forecasting horizon. The x-axis represents the number of epochs during training, while the y-axis represents the validation loss. The validation loss starts high and gradually decreases with each epoch until it stabilizes at around 50 epochs, with a similar final loss as the RNN model.
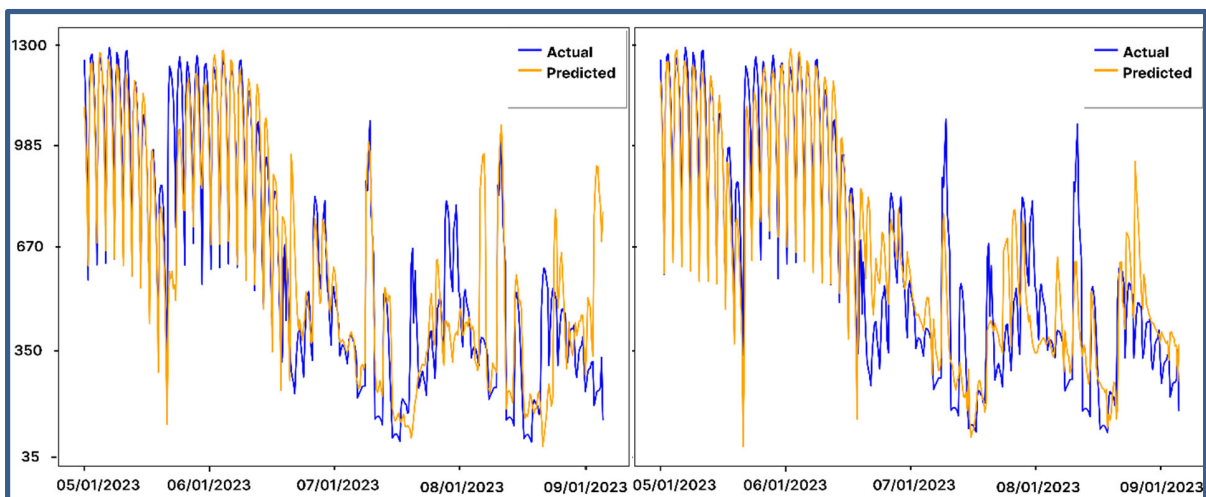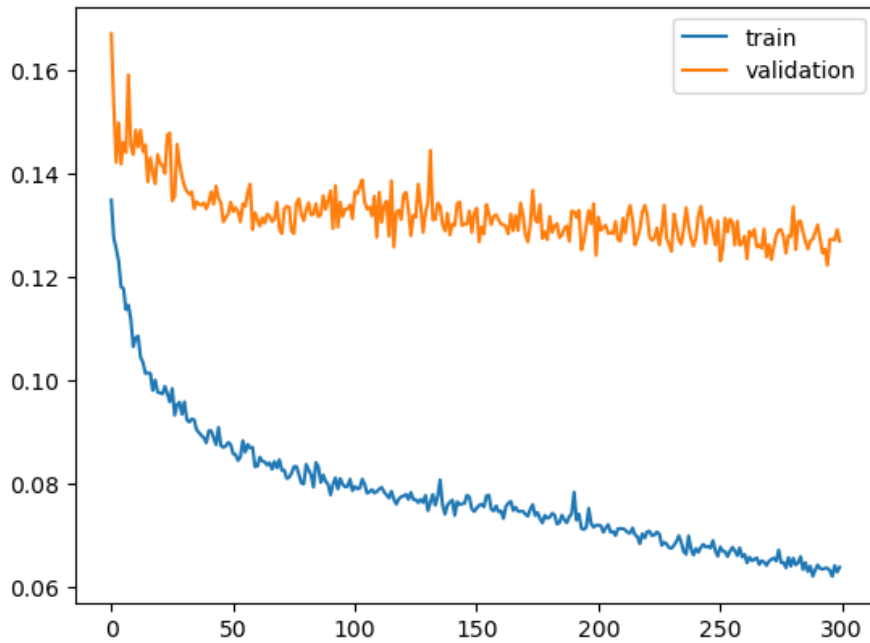
Figure 16. Transformers Training (a) and Validation (b) Graph with Forecasting Horizon 14 (No of Epoch Vs Validation Loss)

RNN Training Graph with Forecasting Horizon 7 (No of Epoch Vs Validation Loss):

RNN Training graph With Forecasting Horizon 7": This graph shows the validation loss of an RNN model trained to predict a 7-step forecasting horizon. The x-axis represents the number of epochs during training, while the y-axis represents the validation loss. The validation loss starts

high and gradually decreases with each epoch until it stabilizes at around 50 epochs, with a lower final loss than the previous two graphs.
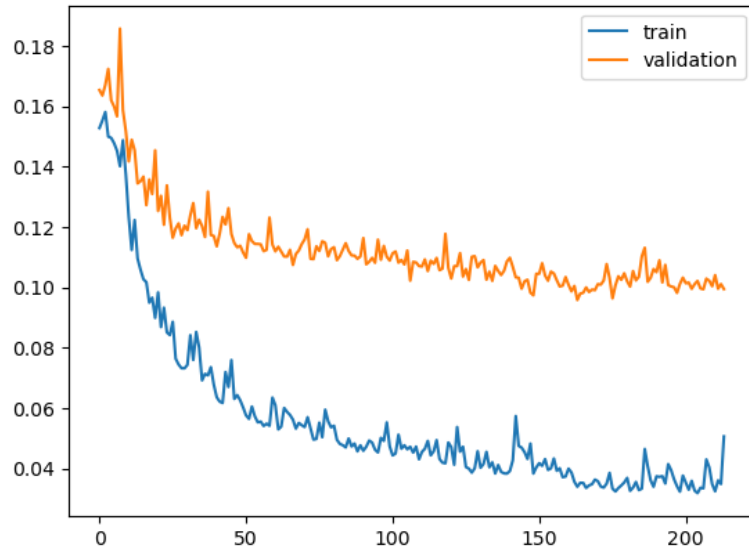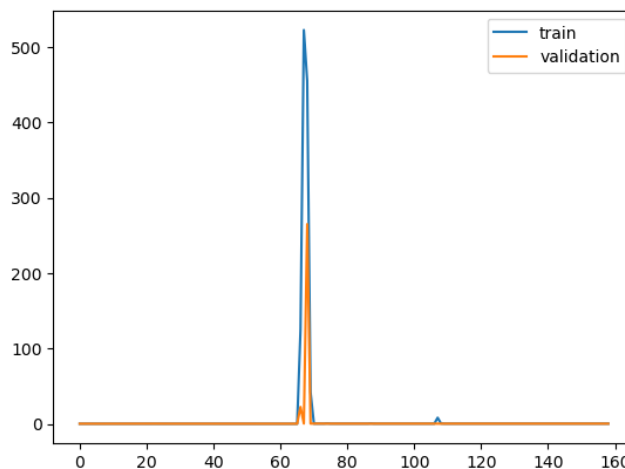

Figure 17. RNN Training Graph with Forecasting Horizon 7 (No of Epoch Vs Validation Loss)

Transformers Training Graph with Forecasting Horizon 7 (No of Epoch Vs Validation Loss):

TRANSFORMERS Training graph With Forecasting Horizon 7": This graph shows the validation loss of a Transformers model trained to predict a 7-step forecasting horizon. The x-axis represents the number of epochs during training, while the y-axis represents the validation loss. The validation loss starts high and gradually decreases with each epoch until it stabilizes at around 50 epochs, with a similar final loss as the RNN model.
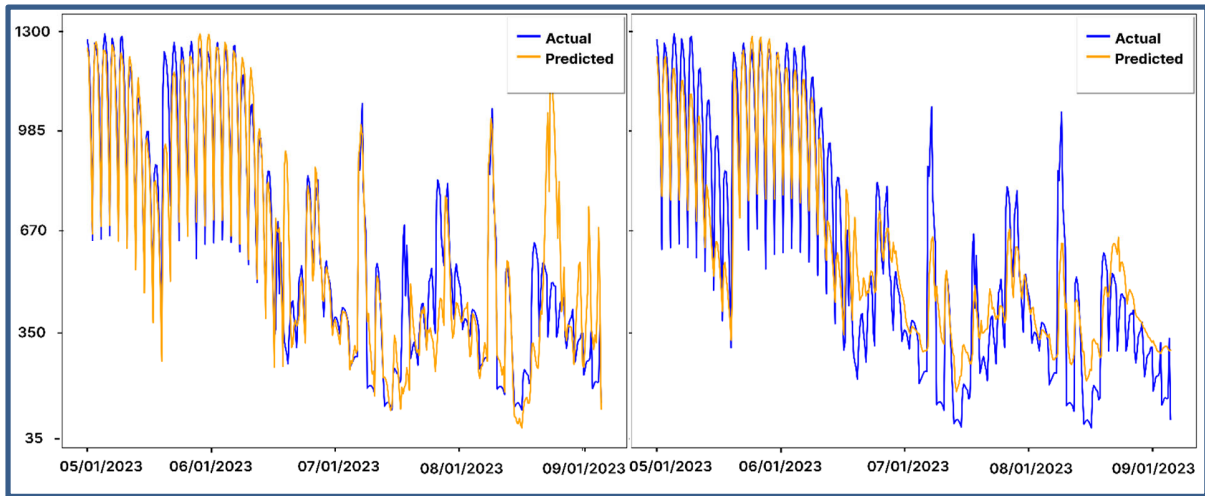
Figure 18. Transformers Training (a) and Validation (b) Graph with Forecasting Horizon 7 (No of Epoch Vs Validation Loss)

RNN Training Graph with Forecasting Horizon 2 (No of Epoch Vs Validation Loss):

RNN Training graph With Forecasting Horizon 2": This graph shows the validation loss of an RNN model trained to predict a 2-step forecasting horizon. The x-axis represents the number of epochs during training, while the y-axis represents the validation loss. The validation loss starts high and gradually decreases with each epoch until it stabilizes at around 50 epochs, with the lowest final loss among all the graphs.
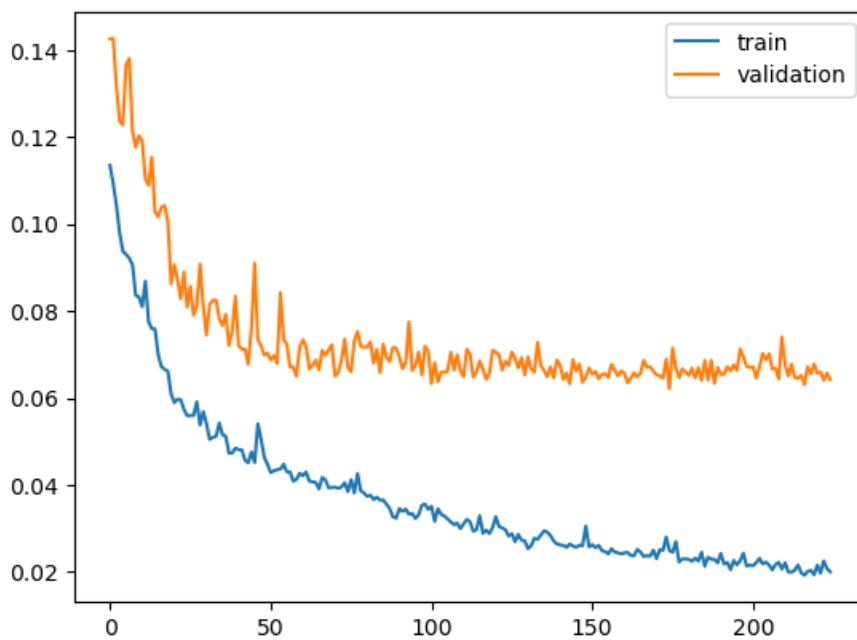

Figure 19. RNN Training Graph with Forecasting Horizon 2 (No of Epoch Vs Validation Loss)

Transformers Training Graph with Forecasting Horizon 2 (No of Epoch Vs Validation Loss):

TRANSFORMERS Training graph With Forecasting Horizon 2": This graph shows the validation loss of a Transformers model trained to predict a 2-step forecasting horizon. The x-axis represents the number of epochs during training, while the y-axis represents the validation loss. The validation loss starts high and gradually decreases with each epoch until it stabilizes at around 50 epochs, with a similar final loss as the RNN model.
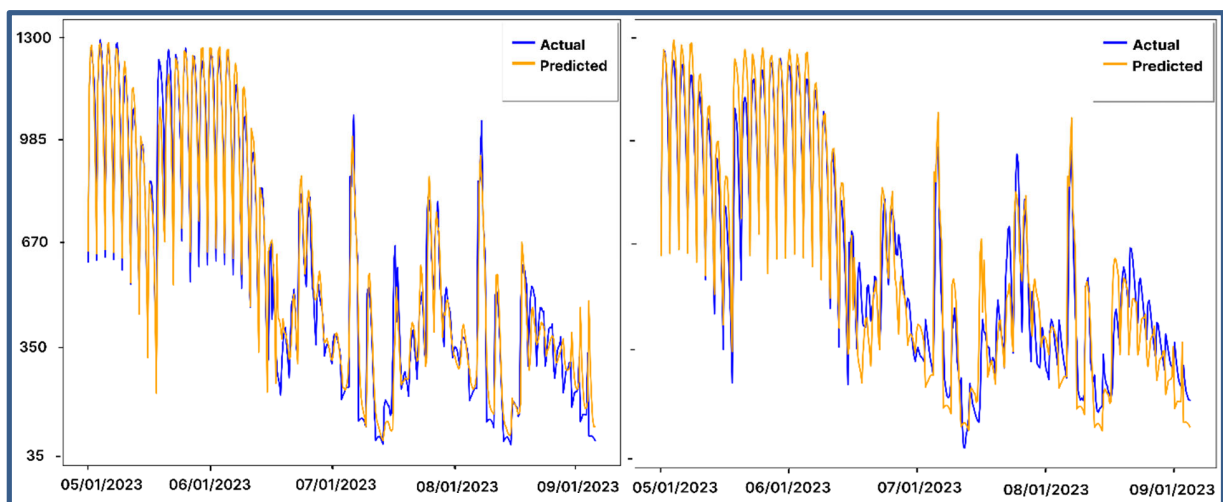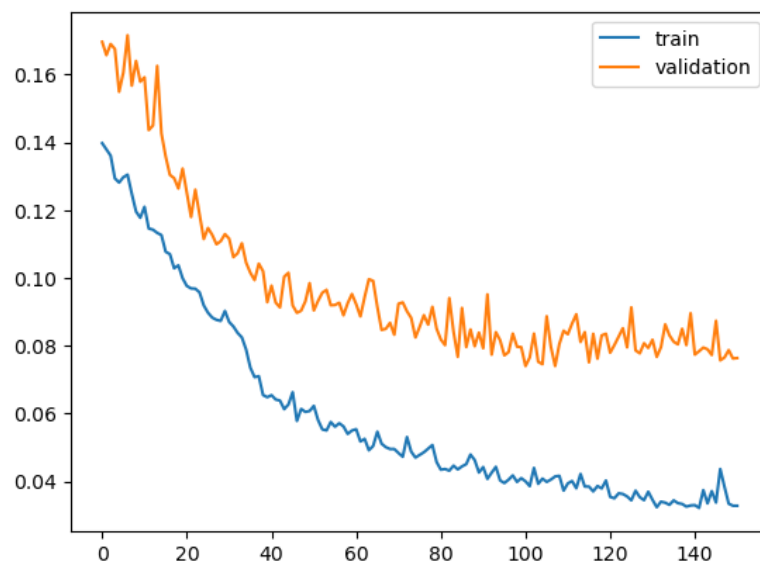

Figure 20. Transformers Training (a) and Validation (b) Graph with Forecasting Horizon 2 (No of Epoch Vs Validation Loss)

CHAPTER 5: CONCLUSION

In conclusion, the results of this study demonstrate the potential of using data-driven methods for forecasting the solar irradiance of bifacial panels in real-time. This approach is particularly useful for achieving the energy performance goals of Nearly Zero Energy Buildings (NZEBs). In the context of refurbishment of existing buildings for NZEBs, the forecasting of solar irradiance can be used to optimize the design and placement of bifacial solar panels. Similarly, in the case of new NZEBs, such forecasting can aid in the selection of sustainable energy technologies, such as bifacial panels, for optimal energy performance. The experimental data used in this study captures the seasonal non-linearity that cannot be accounted for by theoretical models. This is particularly relevant in the context of sustainable energy technologies for NZEBs, where accurate and real-time forecasting is critical for effective energy management. In addition, as urbanization continues to increase, the floor area of buildings increases while the roof area remains constant. This creates an opportunity for bifacial panels to capture more solar energy, making them a desirable technology for NZEBs. The data-driven approach utilized in this study provides a valuable tool for optimizing the energy performance of NZEBs, and can be integrated into the advanced design solutions, optimal control, energy performance assessment, and energy flexibility and demand response strategies of NZEBs. Furthermore, an inclusive approach that considers economic, social, and environmental dimensions of NZEBs can also benefit from accurate and real-time forecasting of solar irradiance for effective energy management. The study also demonstrated that both RNN-LSTM and Transformers models were effective in forecasting irradiance, as evident from the R2 values of 0.927 and 0.894, respectively. Furthermore, the Transformers model performed better than the RNN-LSTM model, with a lower range of MAE values across the same horizons. These results indicate that deep learning models can accurately forecast solar irradiance, which can potentially aid in optimizing the performance of net-zero energy buildings.

APPENDIX A

Cell A

```python
import pandas as pd
from sklearn.preprocessing import MinMaxScaler
import tensorflow as tf
import keras.backend as K
import pandas as pd
import numpy as np
from matplotlib import pyplot as plt
import os
import glob
from matplotlib import pyplot as plt
import seaborn as sns
from numpy import savetxt
from sklearn.preprocessing import MinMaxScaler
from datetime import datetime
from time import time
import json
import logging

import tensorflow as tf
import keras
from keras import layers
from keras.models import Model
from keras.models import load_model
from keras.models import Sequential
from keras.callbacks import EarlyStopping, TensorBoard, ModelCheckpoint
from keras.callbacks import Callback

from kerastuner.tuners import RandomSearch

from sklearn.metrics import r2_score
from datetime import datetime
from time import time
import json
import logging

from keras.utils.vis_utils import plot_model
from keras.utils.vis_utils import model_to_dot

from sklearn.metrics import r2_score

from livelossplot import PlotLossesKeras
```

Cell B

```python
def mape(y_true, y_pred):
    import keras.backend as K
    """
    Returns the mean absolute percentage error.
    For examples on losses see:
    https://github.com/keras-team/keras/blob/master/keras/losses.py
    """
    return (K.abs(y_true - y_pred) / K.abs(y_pred)) * 100
    #diff = K.abs(y_true - y_pred) / K.abs(y_true)
    #return 100. * K.mean(diff)#, axis=-1)

def smape(y_true, y_pred):
    import keras.backend as K
    """
    Returns the Symmetric mean absolute percentage error.
    For examples on losses see:
    https://github.com/keras-team/keras/blob/master/keras/losses.py
    """
    return 100*K.mean(K.abs(y_pred - y_true) / ((K.abs(y_true) + K.abs(y_pred)))),
axis=-1)
    #Symmetric mean absolute percentage error
    #return 100 * K.mean(K.abs(y_pred - y_true) / (K.abs(y_pred) + K.abs(y_true))
)#, axis=-1)

def rmse(y_true, y_pred):
    return K.sqrt(K.mean(K.square(y_pred - y_true)))


def mae(y_true, y_pred):
    n = len(y_pred)
    sum_error = 0
    for i in range(n):
      sum_error += K.abs(y_pred[i] - y_true[i])
    return sum_error / n

def mase(y_true, y_pred):

    sust = K.mean(K.abs(y_true[:,1:] - y_true[:,:-1]))
    diff = K.mean(K.abs(y_pred - y_true))

    return diff/sust

def coeff_determination(y_true, y_pred):

    SS_res =  K.sum(K.square( y_true-y_pred ))
    SS_tot = K.sum(K.square( y_true - K.mean(y_true) ) )
    return ( 1 - SS_res/(SS_tot + K.epsilon()) )

# convert time series to 2D data for supervised learning
def series_to_supervised(data, train_size=0.5, n_in=1, n_out=1, target_column='ta
rget', dropnan=True, scale_X=True):
```

```python
    df = data.copy()

    # Make sure the target column is the last column in the dataframe
    df['target'] = df[target_column] # Make a copy of the target column
    df = df.drop(columns=[target_column]) # Drop the original target column

    target_location = df.shape[1] - 1 # column index number of target

    # ...X
    #X = df.iloc[:, :target_location]
    X = df.iloc[:,:]

    # ...y
    y = df.iloc[:, [target_location]]

    # Scale the features
    if scale_X:
        #col_names=['target']
        #features = X[col_names]
        features = X[X.columns]
        scalerX = MinMaxScaler().fit(features.values)
        features = scalerX.transform(features.values)

        #X['target'] = features
        X[X.columns] = features

    #n_vars_x = X.shape[1]
    x_vars_labels = X.columns
    y_vars_labels = y.columns

    x_cols, x_names = list(), list()
    y_cols, y_names = list(), list()

    # input sequence (t-n, ... t-1)
    for i in range(n_in, 0, -1):
        x_cols.append(X.shift(i))
        x_names += [('%s(t-%d)' % (j, i)) for j in x_vars_labels]

    # forecast sequence (t, t+1, ... t+n)
    for i in range(0, n_out):
        y_cols.append(y.shift(-i))
        if i == 0:
            y_names += [('%s(t)' % (j)) for j in y_vars_labels]
        else:
            y_names += [('%s(t-%d)' % (j, i)) for j in y_vars_labels]

    # put it all together
    x_agg = pd.concat(x_cols, axis=1)
    x_agg.columns = x_names

    y_agg = pd.concat(y_cols, axis=1)
    y_agg.columns = y_names
```

```python
    agg=pd.concat([x_agg,y_agg], axis=1)
    agg.columns = x_names + y_names
    #print(agg)


    # drop rows with NaN values
    if dropnan:
        x_agg.dropna(inplace=True)
        y_agg.dropna(inplace=True)

    # drop rows with NaN values
    if dropnan:
        agg.dropna(inplace=True)

    """
    diff = y_agg.shape[0] - x_agg.shape[0]
    idx = [i for i in range(0, diff)]
    y_agg = y_agg.drop(df.index[idx])"""

    nf = X.shape[1]
    xx = agg.iloc[:,:n_in*nf]
    yy = agg.iloc[:,-n_out:]

    split_index = int(xx.shape[0]*train_size) # the index at which to split df in
to train and test

    # ...train
    X_train = xx.iloc[:split_index, :]
    y_train = yy.iloc[:split_index, ]

    # ...test
    X_test = xx.iloc[split_index:, :] # original is split_index:-1
    y_test = yy.iloc[split_index:, ] # original is split_index:-1

    # ...CV
    split_cv = int(X_test.shape[0]*0.5)
    x_cv = X_test.iloc[:split_cv,]
    x_test = X_test.iloc[split_cv:,]
    y_cv = y_test.iloc[:split_cv,]
    y_test = y_test.iloc[split_cv:,]

    return X_train, y_train, x_test, y_test, x_cv, y_cv, scale_X
```

Cell C

```python
callback_history = rnn.train(X_train_reshaped,y_train_reshaped,x_cv_reshaped,
                             y_cv_reshaped, epochs=300 ,batch_size=51)

_, rmse_result, mae_result, smape_result, r2_result, y_pred = rnn.evaluate(X_test_res
haped,y_test_reshaped)

print('Result \n RMSE = %.2f [C] \n MAE = %.2f [C]\n R2 = %.1f [%%]' % (rmse_result,
                                                        mae_resul
t,
                                                        r2_result
*100))

plt.plot(callback_history.history['loss'], label='train')
plt.plot(callback_history.history['val_loss'], label='validation')
plt.legend()
plt.show()

plt.plot(callback_history.history['coeff_determination'], label='r2', color = 'y')
plt.show()

plt.plot(callback_history.history['rmse'], color = 'y')
plt.show()

plt.plot(callback_history.history['mae'], label='mae', color = 'y')
plt.show()


print(y_pred.shape)
print(y_test.shape)

test= np.array(y_test)
pred = np.array(y_pred)

plt.figure(figsize=(10,8),dpi=500)
plt.plot( test[0:417,0], color='blue', label='Predicted')
plt.plot( pred[0:417,0], color='orange', label='Actual')
plt.xlabel('Time')
plt.ylabel('Target Value')
plt.legend()
plt.show()



plt.figure(figsize=(10,8),dpi=500)
plt.plot( pred[0:417,0], color='orange', label='Actual')
plt.plot( test[0:417,0], color='blue', label='Predicted')
plt.xlabel('Time')
plt.ylabel('Target Value')
plt.legend()
plt.show()
```

REFERENCES

[1]   K. Obaideen et al., "On the contribution of solar energy to sustainable developments goals: Case study on Mohammed bin Rashid Al Maktoum Solar Park," International Journal of Thermofluids, vol. 12, Nov. 2021, doi: 10.1016/J.IJFT.2021.100123.

[2]   I. Pence, R. Yıldırım, M. Siseci Cesmeli, A. Güngör, and A. Akyüz, "Evaluation of machine learning approaches for estimating thermodynamic properties of new generation refrigerant R513A," Sustainable Energy Technologies and Assessments, vol. 55, Feb. 2023, doi: 10.1016/J.SETA.2022.102973.

[3]   S. Gawusu et al., "Renewable energy sources from the perspective of blockchain integration: From theory to application," Sustainable Energy Technologies and Assessments, vol. 52, Aug. 2022, doi: 10.1016/J.SETA.2022.102108.

[4]   M. A. Russo, D. Carvalho, N. Martins, and A. Monteiro, "Forecasting the inevitable: A review on the impacts of climate change on renewable energy resources," Sustainable Energy Technologies and Assessments, vol. 52, Aug. 2022, doi: 10.1016/J.SETA.2022.102283.

[5]   R. R. Dias, M. C. Deprá, I. A. Severo, L. Q. Zepka, and E. Jacob-Lopes, "Smart override of the energy matrix in commercial microalgae facilities: A transition path to a low-carbon bioeconomy," Sustainable Energy Technologies and Assessments, vol. 52, Aug. 2022, doi: 10.1016/J.SETA.2022.102073.

[6]   K. Almutairi et al., "Performance optimization of a new flash-binary geothermal cycle for power/hydrogen production with zeotropic fluid," vol. 145, pp. 1633–1650, 2021, doi: 10.1007/s10973-021-10868-2.

[7]   T. Salameh, E. T. Sayed, M. A. Abdelkareem, A. G. Olabi, and H. Rezk, "Optimal selection and management of hybrid renewable energy System: Neom city as a case study," Energy Convers Manag, vol. 244, Sep. 2021, doi: 10.1016/j.enconman.2021.114434.

[8]   A. Sharif, M. S. Meo, M. A. F. Chowdhury, and K. Sohag, "Role of solar energy in reducing ecological footprints: An empirical analysis," J Clean Prod, vol. 292, Apr. 2021, doi: 10.1016/J.JCLEPRO.2021.126028.

[9]   F. M. Guangul and G. T. Chala, "Solar Energy as Renewable Energy Source: SWOT Analysis; Solar Energy as Renewable Energy Source: SWOT Analysis," 2019 4th MEC International Conference on Big Data and Smart City (ICBDSC), 2019.

[10]   H. Weldekidan, V. Strezov, and G. Town, "Review of solar energy for biofuel extraction," Renewable and Sustainable Energy Reviews, vol. 88, pp. 184–192, May 2018, doi: 10.1016/J.RSER.2018.02.027.

[11]   T. Tsoutsos, N. Frantzeskaki, and V. Gekas, "Environmental impacts from the solar energy technologies," Energy Policy, vol. 33, no. 3, pp. 289–296, Feb. 2005, doi: 10.1016/S0301-4215(03)00241-6.

[12]   E. Kabir, P. Kumar, S. Kumar, A. A. Adelodun, and K. H. Kim, "Solar energy: Potential and future prospects," Renewable and Sustainable Energy Reviews, vol. 82, pp. 894–900, 2018, doi: 10.1016/J.RSER.2017.09.094.

[13]   K. H. Solangi, M. R. Islam, R. Saidur, N. A. Rahim, and H. Fayaz, "A review on global solar energy policy," Renewable and Sustainable Energy Reviews, vol. 15, no. 4, pp. 2149–2163, May 2011, doi: 10.1016/J.RSER.2011.01.007.

[14]   R. Saidur, M. R. Islam, N. A. Rahim, and K. H. Solangi, "A review on global wind energy policy," Renewable and Sustainable Energy Reviews, vol. 14, no. 7, pp. 1744–1762, 2010, doi: 10.1016/J.RSER.2010.03.007.

[15]   S. A. Haider, M. Sajid, and S. Iqbal, "Forecasting hydrogen production potential in islamabad from solar energy using water electrolysis," Int J Hydrogen Energy, vol. 46, no. 2, pp. 1671–1681, Jan. 2021, doi: 10.1016/J.IJHYDENE.2020.10.059.

[16]   N. Niveditha and M. M. Rajan Singaravel, "Optimal sizing of hybrid PV–Wind–Battery storage system for Net Zero Energy Buildings to reduce grid burden," Appl Energy, vol. 324, Oct. 2022, doi: 10.1016/J.APENERGY.2022.119713.

[17]   R. Guerrero-Lemus, R. Vega, T. Kim, A. Kimm, and L. E. Shephard, "Bifacial solar photovoltaics-A technology review," 2016, doi: 10.1016/j.rser.2016.03.041.

[18]   A. M. Soomar, A. Hakeem, M. Messaoudi, P. Musznicki, A. Iqbal, and S. Czapp, "Solar Photovoltaic Energy Optimization and Challenges," Front Energy Res, vol. 10, p. 445, May 2022, doi: 10.3389/FENRG.2022.879985/TEXT.

[19]   S. Iqbal, S. N. Khan, M. Sajid, J. Khan, Y. Ayaz, and A. Waqas, "Impact and performance efficiency analysis of grid-tied solar photovoltaic system based on installation site environmental factors," https://doi.org/10.1177/0958305X221106618, Jun. 2022, doi: 10.1177/0958305X221106618.

[20]   A. Desai, I. Mukhopadhyay, and A. Ray, "Feasibility Assessment of Bifacial Rooftop Photovoltaic Systems in the State of Gujarat in India," Front Energy Res, vol. 10, p. 620, Jun. 2022, doi: 10.3389/FENRG.2022.869890/BIBTEX.

[21]   H. Ren, Z. Ma, A. B. Chan, and Y. Sun, "Optimal planning of municipal-scale distributed rooftop photovoltaic systems with maximized solar energy generation under constraints in high-density cities," Energy, vol. 263, Jan. 2023, doi: 10.1016/J.ENERGY.2022.125686.

[22]   R. Kopecek and J. Libal, "Bifacial Photovoltaics 2021: Status, Opportunities and Challenges," Energies 2021, Vol. 14, Page 2076, vol. 14, no. 8, p. 2076, Apr. 2021, doi: 10.3390/EN14082076.

[23]   Y. Wang, C. Yanarates, and Z. Zhou, "External Current Source–Based Unilluminated PV Partial Shading Emulation System Verified Through the Hybrid Global Search Adaptive Perturb and Observe MPPT Algorithm," Front Energy Res, vol. 10, p. 281, Apr. 2022, doi: 10.3389/FENRG.2022.868951/BIBTEX.

[24]   A. Agwa, A. M. Agwa, and I. Y. Mahmoud, "Photovoltaic Maximum Power Point Tracking by Artificial Neural Networks," 2017. [Online]. Available: https://www.researchgate.net/publication/336145182

[25]   X. Sun, M. R. Khan, C. Deline, and M. A. Alam, "Optimization and performance of bifacial solar modules: A global perspective," Appl Energy, vol. 212, pp. 1601–1610, Feb. 2018, doi: 10.1016/j.apenergy.2017.12.041.

[26]   W. Gu, T. Ma, M. Li, L. Shen, and Y. Zhang, "A coupled optical-electrical-thermal model of the bifacial photovoltaic module," Appl Energy, vol. 258, p. 114075, Jan. 2020, doi: 10.1016/J.APENERGY.2019.114075.

[27]   S. A. Haider, M. Sajid, H. Sajid, E. Uddin, and Y. Ayaz, "Deep learning and statistical methods for short- and long-term solar irradiance forecasting for Islamabad," Renew Energy, vol. 198, pp. 51–60, Oct. 2022, doi: 10.1016/J.RENENE.2022.07.136.

[28]   M. A. H. Shah, H. Butt, M. Farooq, M. N. Ihsan, M. Sajid, and E. Uddin, "Development of a truncated ellipsoidal reflector-based metal halide lamp solar simulator for characterization of photovoltaic cells," Energy Sources, Part A: Recovery, Utilization and Environmental Effects, vol. 43, no. 20, pp. 2554–2568, 2021, doi: 10.1080/15567036.2020.1842557.

[29]   B. Rasheed, A. Safdar, M. Sajid, S. Ali, and Y. Ayaz, "Assessment of solar load models for bifacial PV panels," Front Energy Res, vol. 10, p. 1730, Nov. 2022, doi: 10.3389/FENRG.2022.1019595/BIBTEX.

[30]   A. Desai, I. Mukhopadhyay, and A. Ray, "Feasibility Assessment of Bifacial Rooftop Photovoltaic Systems in the State of Gujarat in India," Front Energy Res, vol. 10, p. 620, Jun. 2022, doi: 10.3389/FENRG.2022.869890/BIBTEX.

[31]   S. A. Pelaez and C. Deline, "bifacial_radiance: a python package for modeling bifacial solar photovoltaic systems," J Open Source Softw, vol. 5, no. 50, p. 1865, Jun. 2020, doi: 10.21105/JOSS.01865.

[32]   W. Jiang et al., "Net-zero energy optimization of solar greenhouses in severe cold climate using passive insulation and photovoltaic," J Clean Prod, p. 136770, May 2023, doi: 10.1016/J.JCLEPRO.2023.136770.

[33]   A. Alzahrani, P. Shamsi, M. Ferdowsi, and C. Dagli, "Solar irradiance forecasting using deep recurrent neural networks," 2017 6th International Conference on Renewable Energy Research and Applications, ICRERA 2017, vol. 2017-January, pp. 988–994, Dec. 2017, doi: 10.1109/ICRERA.2017.8191206.

[34]   W.-H. Lin et al., "Wind Power Forecasting with Deep Learning Networks: Time-Series Forecasting," Applied Sciences 2021, Vol. 11, Page 10335, vol. 11, no. 21, p. 10335, Nov. 2021, doi: 10.3390/APP112110335.

[35]   S. Ahmed, I. E. Nielsen, A. Tripathi, S. Siddiqui, G. Rasool, and R. P. Ramachandran, "Transformers in Time-series Analysis: A Tutorial," Apr. 2022, Accessed: Mar. 31, 2023. [Online]. Available: http://arxiv.org/abs/2205.01138

[36]   A. Vaswani et al., "Attention Is All You Need," Jun. 2017, [Online]. Available: http://arxiv.org/abs/1706.03762

[37]   J. Chung, C. Gulcehre, K. Cho, and Y. Bengio, "Empirical Evaluation of Gated Recurrent Neural Networks on Sequence Modeling," Dec. 2014, Accessed: Mar. 31, 2023. [Online]. Available: https://arxiv.org/abs/1412.3555v1

[38]   "GitHub - keras-team/keras-tuner: A Hyperparameter Tuning Library for Keras." https://github.com/keras-team/keras-tuner (accessed Mar. 30, 2023).

Junaid Iqbal 362035 Thesis Report

7 Yathin Krishna, Shashikantha Karinka, Mohd Faizal Fauzan, Prashanth Pai Manihalla. "An Experimental and Mathematical investigation of optimal tilt angle and effects of reflectors on PV energy production", MATEC Web of Conferences, 2021
Publication

1%

8 Bushra Rasheed, Asmara Safdar, Muhammad Sajid, Sara Ali, Yasar Ayaz. "Assessment of solar load models for bifacial PV panels", Frontiers in Energy Research, 2022
Publication

1%

Exclude quotes	Off	Exclude matches	< 1%
Exclude bibliography	On		